applied sciences

MDPI

Review

Fluid Flow-Based Vibration Energy Harvesters: A Critical Review of State-of-the-Art Technologies

Sadia Bakhtiar [1], Farid Ullah Khan [2], Hailing Fu [3], Amal Z. Hajjaj [1] and Stephanos Theodossiades [1,*]

[1] Wolfson School of Mechanical, Electrical and Manufacturing Engineering, Loughborough University, Loughborough LE11 3TU, UK; s.bakhtiar@lboro.ac.uk (S.B.); a.a.hajjaj@lboro.ac.uk (A.Z.H.)
[2] Department of Mechatronics Engineering, University of Engineering and Technology, Peshawar 25000, Pakistan; dr_farid_khan@uetpeshawar.edu.pk
[3] School of Automation, Beijing Institute of Technology, Beijing 100081, China; hailing.fu@bit.edu.cn
* Correspondence: s.theodossiades@lboro.ac.uk

Abstract: Energy harvesting technology plays an important role in converting ambient energy into useful electrical energy to power wireless sensing and system monitoring, especially for systems operating in isolated, abandoned or embedded locations where battery replacement or recharging is not a feasible solution. This paper provides an integrative study of the methodologies and technologies of energy harvesting from fluid flow-induced vibration (FIV). The recent research endeavors contributing to flow-based energy harvesting have been reviewed to present the state-of-the-art issues and challenges. Several mechanisms on FIVs including vortex-induced vibrations (VIVs), flutter, galloping and wake galloping are thoroughly discussed in terms of device architecture, operating principles, energy transduction, voltage production and power generation. Additionally, advantages and disadvantages of each FIV energy harvesting mechanism are also talked about. Power enhancement methods, such as induced nonlinearities, optimized harvester's configuration, hybridization and coupling of aerodynamic instabilities, for boosting the harvester's output are also elucidated and categorized. Moreover, rotary wind energy harvesters are reviewed and discussed. Finally, the challenges and potential directions related to the flow-based energy harvesters (FBEHs) are also mentioned to provide an insight to researchers on the development of sustainable energy solutions for remote wireless sensing and monitoring systems.

Keywords: aerodynamics; electromagnetic; flow energy harvester; flow-induced vibrations; flutter; galloping; piezoelectric; Karman vortex street; nonlinear; rotary; triboelectric; vortex-induced vibrations; wake galloping

Citation: Bakhtiar, S.; Khan, F.U.; Fu, H.; Hajjaj, A.Z.; Theodossiades, S. Fluid Flow-Based Vibration Energy Harvesters: A Critical Review of State-of-the-Art Technologies. *Appl. Sci.* **2024**, *14*, 11452. https://doi.org/10.3390/app142311452

Academic Editor: Alessandro Lo Schiavo

Received: 31 October 2024
Revised: 26 November 2024
Accepted: 27 November 2024
Published: 9 December 2024

1. Introduction

With the recent advancements in low-power sensors and efficient wireless communication technologies, the application of autonomous systems and the Internet of Things (IoT) have become more prominent and are now commonly used in condition monitoring, traffic maintenance, supervision of industrial equipment and machines, surveillance of defense and military tracking systems and structural health monitoring [1,2]. Wireless sensor nodes (WSNs) function mostly as distributed autonomous sensors capable of sensing and monitoring physical and environmental conditions. However, low-power WSNs are still in the early stages of research and encounter several challenges. The WSNs require electric power to receive and transmit signals for sensing and monitoring purposes. Although large batteries could be used due to the small size of WSNs, they are not a suitable option. Therefore, technology that harnesses environmental energy is generally targeted for achieving the goal of an in situ free energy source for operation of WSNs. Moreover, the size and power requirements of electronic devices and gadgets are swiftly shrinking; therefore, the energy harvesting technology has the potential to provide an alternative energy source for self-powered applications [3,4]. The energy harvesters utilize ambient

energy and provide a self-sufficient, sustainable power source for ultra-low power devices like portable electronics, wearable devices and WSNs [5,6]. With the ever-growing demand for data collection and processing along continuous monitoring for long periods of IoT applications in heterogenous environments, WSNs installed in distant and remote sites like deserts, forests and marine environments require integration with energy harvesters to operate these autonomously as self-powered systems. Some commercially available wireless sensors are shown in Table 1, where data were taken from specification sheets, which can be found on the websites of the manufacturers. In general, a voltage of 2–5 V is needed for the operation of these sensors. Furthermore, the current consumed by the sensors while transmitting data ranges from 2.8 µA to 15 mA overall.

Table 1. Operating features of commercially available sensors.

Wireless Sensors	Company	Model Type	Measurement Range	Supply Voltage (V)	Supply Current (mA)
Pressure	MICROSENSOR Corporation, ShanXi, China	MPM286	20–3500 kPa		2.0
	Freescale Semiconductor, Austin, TX, USA	MXP 5700	0–700 kPa	5	10
	ALTHEN Sensors and Control, Belgium, The Netherlands	MDM6861	0–35 kPa	3.6	-
	HOLYKELL, HuNan, China	H2600 SERIES	1–100 MPa	3.6	
Temperature	MONNIT, Salt Lake City, UT, USA	ZTL-G2SC1	−40–85 °C	3	2.5
	ALTHEN Sensors and Control, Belgium, The Netherlands	MDM6861	−50–150 °C	3.6	-
	TEXAS Instruments, Dallas, TX, USA	TMP100	−55–125 °C	2.7	0.075
	TEXAS Instruments, Dallas, TX, USA	LM61	−25–85 °C	2.7	0.125
Flow	FLUIGENT, Ile-de-France, France	FRP	7 nL/min–5 mL/min.	-	-
	MICROCHIP, Chandler, AZ, USA	YF-S201	1–30 L/min	4.5	15
	OMEGA, Norwalk, CT, USA	FD-400	0.05–9.14 m/s	5	-
	Spire Metering Technology, New Jersey, NJ, USA	EF10	−10–10 m/s	-	-
Humidity	OMEGA, Norwalk, CT, USA	UWRH2	2–98% RH	3.6	
	MONNIT, Salt Lake City, UT, USA	MNS2-9W1-HU-RH	0–100% RH	3	2.5
Combined Humidity, Pressure and Temperature Sensor	BOSCH, Gerlingen, Germany	BME280	For humidity: 0–100% RH For pressure: 300–1100 hPa For temperature: −40–85 °C	3.6	For humidity and temperature 0.0028 For pressure: 0.0042
Humidity and Temperature Sensor	SENSIRION, Stäfa, Switzerland	SHT3x-DIS	For humidity: 0–100% RH For temperature: −40–125 °C	2.5–5.5	1.5
Humidity and Temperature Sensor	SILICON LABS, Austin, TX, USA	Si7020-A20	For humidity: 0–100% RH For temperature: −40–125 °C	3.6	For humidity: 0.18 For temperature: 0.12

In the surroundings of WSNs, numerous modes of ambient energy are present which can be potentially converted to useful electricity. This ambient energy is a source of usable and harvestable energy as it offers a green and theoretically unlimited resource. Ambient energy sources present in the environment are in different forms, such as acoustic [7], chemical [8], wind [9], thermal [10], solar [11] and mechanical vibration [12]. Even though, in comparison to other energy sources, mechanical vibration energy is almost always

present in the environment, the frequency range and level of acceleration are widely different and depend on the source of environmental vibration [13]. Therefore, it is crucial to develop energy harvesting techniques that can adapt to changing vibration conditions. Nature provides abundant wind energy, which is regarded as one of the most promising substitutes for fossil fuels [14]. Wind energy, which is one of the most prevalent sources of energy on Earth, has gained interest globally and has been the subject of research studies due to its renewability, cleanliness, and availability.

The investigation of flow-induced vibrations (FIVs) phenomena, driven by well-established energy harvesting technology, has been motivated in terms of their potential of conversion of fluidic kinetic energy from both wind and water circulation systems [15]. Figure 1 outlines various scenarios for wind and water energy sources. These range from metropolitan environments with high-rise buildings and subway stations to rural locations and coastal regions. The kinetic energy from the ocean waves and gushing winds can be harvested with mesoscale rotary turbines or with FIV energy harvesters.

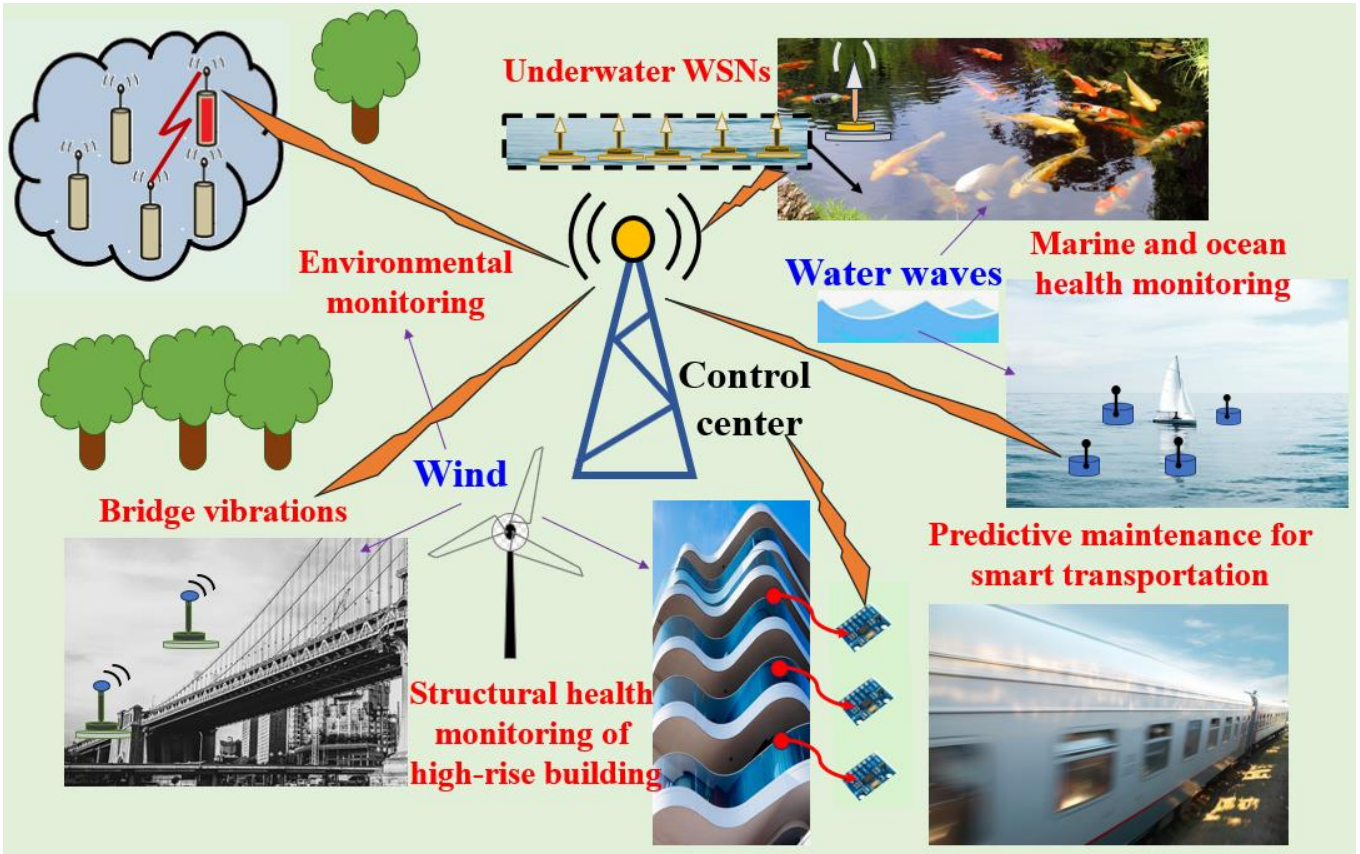

Figure 1. Potential energy sources for FIV-based harvesting for powering WSNs in IoT applications.

Recognizing the substantial research advancements in the field of FIV energy harvesters, rapid progress is driven towards sustainable energy solutions for powering WSNs. The ambient fluid flow [16–18] is in abundance in day-to-day life and industrial environment. Flow-based energy harvesters (FBEHs) are developed to take advantage of flow-induced structural vibrations generated by the natural fluid flow when encountering obstacles in the flow field. The fluid structure interaction (FSI) produces aerodynamic effects, variations in air pressure and velocity over time which cause oscillatory patterns in the flow. The FIVs for energy harvesting can be split into distinct vibration mechanisms such as vortex-induced vibrations (VIVs) [19], flutter [20], galloping [21] and wake galloping [22]. These mechanisms refer to aeroelastic instabilities. These instabilities are caused by the interaction of the harvester's structure with the wind flow. However, in some cases

turbulence-induced vibrations [23,24], which are caused by pressure fluctuations in the airflow, are utilized. Based on aeroelastic instabilities, the power generation process incorporates the aero-electro-mechanical coupling comprising the integration of fluid dynamics, structural dynamics and electricity. The nonlinear aerodynamic force sets up mechanical vibrations through the fluid–structure coupling, which are subsequently converted into electrical energy by the harvester's transduction mechanism [25].

In this paper, a comprehensive review is conducted on FBEHs developed to power WSNs in IoT-based monitoring systems. Fundamental concepts and aerodynamic instabilities (VIVs, flutter, galloping and wake galloping) are discussed. A detailed comparison of energy harvesting devices offers insights into optimizing wind energy harvesting technologies. It extensively covers different energy transduction mechanisms such as piezoelectric (PE), electromagnetic (EM) and triboelectric (TE), and moreover highlights their performance and applicability. Likewise, hybrid energy harvesters are also discussed that incorporate more than one energy transduction method, along with harvesters based on coupled fluid phenomena, highlighting how these innovative designs enhance energy conversion and overall performance. In addition, nonlinearities introduced in FIV energy harvesters are thoroughly examined, covering each flow-induced mechanism and transduction technique employed. Additionally, common wind-driven rotary energy harvesters are reviewed, emphasizing their usefulness and practicality for powering monitoring sensors. This paper not only highlights the advantages and practical applications but also indicates the limitations of flow energy harvesters regarding their transduction mechanisms and ways to improve performance. Finally, strategies to enhance power output and key challenges related to FBEHs are debated.

2. Flow-Induced Vibrations (FIVs) and Energy Harvesting

FIVs phenomena are caused by various aerodynamic instabilities classified as VIVs, galloping, flutter and wake galloping, each of which results in distinct aeroelastic response, with galloping and VIV being widely explored for energy harvesting. The power generation process from these aeroelastic instabilities encompasses the combined effects of fluid forces, mechanical coupling with the device structure (described as FSI) and the energy transduction mechanism utilized in the device. The interaction of these three research areas necessitates a highly interdisciplinary approach, as illustrated in Figure 2. Researchers in fluid dynamics, structural mechanics and electrical engineering interact to design systems that can effectively harvest energy from aeroelastic instabilities into useful electricity. This is especially useful in scenarios where standard wind or water turbines are impractical.

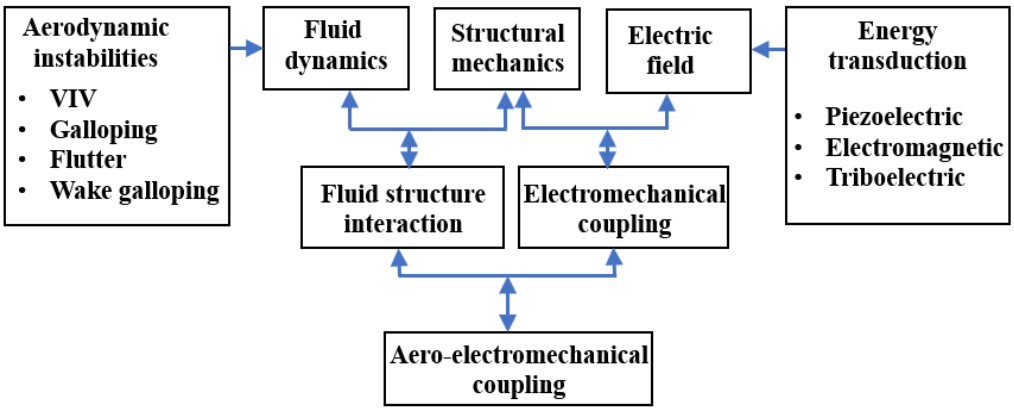

Figure 2. Schematic of coupling between fluid, structure and energy transduction in FBEHs.

2.1. Aeroelastic Instability and Structural Dynamics

FSI is the interplay of fluid dynamics with structural mechanics. It is challenging due to its intrinsic nonlinearity. The quasi-steady theory [21] is frequently adopted for the simplification of fluid–structure interaction problems. It assumes that at any instant of time

when a structure is subjected to ambient fluid flow, it is in steady state, ignoring the transient conditions due to the motion induced in the structure. This theory approximates the same time scales for both the fluid and the structure. Based on this approach, simulations and experiments can be conducted to analyze the effects of fluid flow on the structure. This relationship, however, also depends on the cross-sectional geometry and surface roughness of the structure [26]. These structures are mentioned as bluff bodies in the field of FIVs. In addition to the aerodynamic load determined by the bluff body, the FIV is affected by the dynamics of the elastic structures in FBEHs. As a result, numerous novel topologies for FIV energy harvesting have been developed and reported.

2.2. Energy Transduction in Flow Energy Harvesting

The typical FIV energy harvester in accordance with the various energy transduction techniques can be classified into electromagnetic [27,28], piezoelectric [29], triboelectric [30] and hybrid [31]. Out of these techniques, piezoelectric transduction has gained a lot of attention due to high voltage output, simplicity of device architecture and independence from an external magnetic field or voltage sources. Piezoelectric materials develop an electric polarization when these experience mechanical strain. As the applied stress causes the displacement of charge within the material, this leads to a separation of positive and negative charges, generating voltage across the material. Piezoelectric materials are well suited to MEMS fabrication techniques, which can significantly reduce the overall device size. So far, such self-powered piezoelectric devices are tiny, implanted sensors releasing wireless signals utilized to evaluate the performance of mechanical systems. Moreover, because of fewer moving components, it is less likely to need maintenance [32,33]. Another method for harvesting energy from FIVs is to use electromagnetic induction [34–36] to transform mechanical energy from ambient vibration into electrical energy. The fundamental concept of an electromagnetic energy harvester (EMEH) is that as a magnet and coil undergo relative motion, the varying amounts of magnetic flux through the coil generate voltage. Although EMEHs have high power output levels, they generate comparatively low voltage when used on a small scale. Furthermore, triboelectric energy harvesting has received substantial interest in recent years due to their low cost, triboelectric effect diversity, high efficiency and robustness. Triboelectric flow energy harvesters utilize the triboelectric effect, i.e., contact-induced electrification in which a material electrifies itself after coming into frictional contact with another material. These can capture a wide range of mechanical energy, including vibration, impact, touching, linear sliding, rotation, wind and human motion [37,38].

Recent research on FIV energy harvesting shows improvements in the comprehension of energy transduction mechanisms for transforming mechanical vibrations into electrical energy. Critical analysis, however, exposes difficulties, such as constrained scalability, sensitivity to flow conditions and efficiency issues. To address these gaps, advancement of efficient FIV energy harvesting systems should be encouraged, giving priority to developing scalable, sustainable solutions that are more adaptable to a wider range of flow conditions and have increased efficiency.

3. Karman Vortex Street-Based Energy Harvesting

A Kármán vortex street (or a von Kármán vortex street) is a recurring pattern of whirling vortices created by vortex shedding, which is responsible for the unstable separation of flow around obstacles [39]. When fluid is flowing around the bluff body, a vortex is formed in the path behind the bluff body periodically. The vortex's shedding frequency, $f = \frac{uS_t}{L}$, depends on the Strouhal number S_t (taken as a constant within a given Reynolds number range), the characteristic length L and the incoming flow velocity u. The vortex that is formed behind the bluff body creates an asymmetric pressure field around it, which is subsequently exposed to alternating aerodynamic forces, resulting in vibrations of the bluff body with limited amplitude. When the vortex shedding frequency is near to the bluff body's natural frequency, resonance takes place, and the bluff body vibrates with large

amplitude. At the same time, the phenomenon of frequency lock-in may occur, usually known as the synchronization region, as illustrated in Figure 3a, where the frequency of vortex shedding will no longer fluctuate with the flow velocity within a given range of incoming flow velocities [40]. Such unsteady fluid flows in the wake behind a cylinder are called Karman vortex streets, as depicted in Figure 3b. They consist of a wobbled group of vortices which shed periodically and rotate in alternating directions, both at the top and bottom of the cylinder.

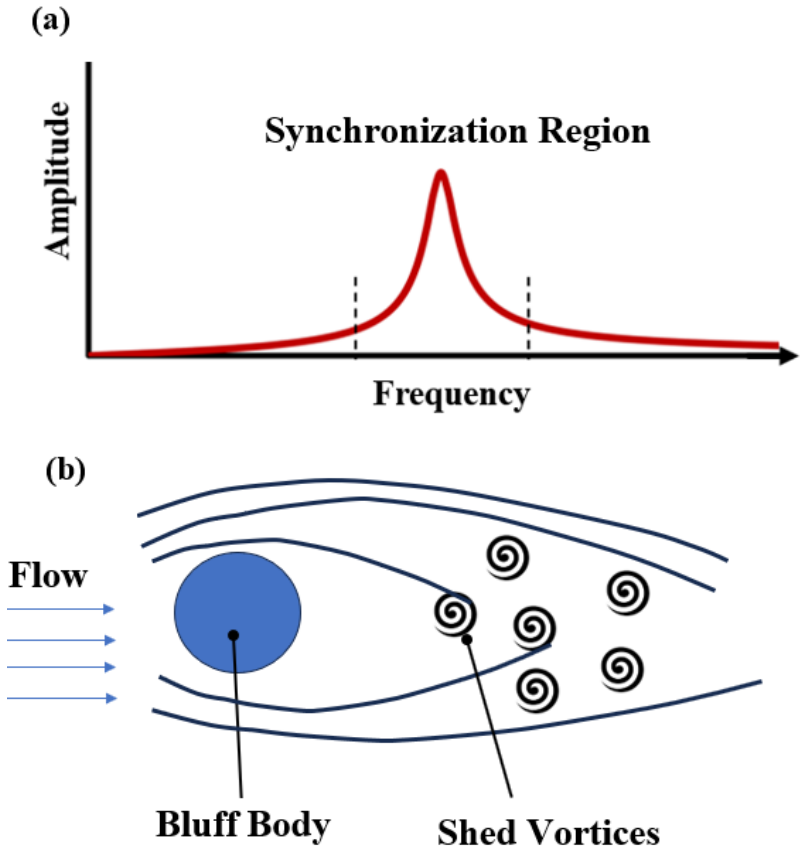

Figure 3. Typical trend of VIVs: (**a**) synchronization region; (**b**) Karman vortex street.

3.1. Karman Vortex Street-Based PE-FBEHs

Akaydin et al. [41] utilized piezoelectric harvesters to investigate various attributes of energy harvesting from unstable and turbulent flows. A beam with piezoelectric material was placed in the Karman vortex street, with the static pressure on the beam altered dynamically, causing the beam to oscillate. A lift force is generated by the vortex formation. The voltage induced by piezoelectric beams that were positioned in the wakes of a turbulent flow of circular cylinders at high Reynolds numbers was examined. Wang et al. [39] developed PE-FBEHs for harvesting energy from the VIVs established in the water flow due to the presence of a bluff body. The experimental results showed that an open circuit peak-to-peak output voltage and power of 0.12 V and 0.7 nW are produced, respectively. An optimization design method or the use of a piezoelectric material with higher piezoelectric constants can improve the device's low output power. The study in [42] presents a PE-FBEH comprising a Lead Zirconate Titanate (PZT) beam with a cylinder. At a resonant vibration velocity of 0.35 m/s and optimum resistance range (100–150 kΩ), output power of 84.49 μW was obtained which corresponds to an energy density of 60.35 mW/m^2. The authors concluded that optimizing the mass and diameter of the cylinder can improve the efficiency of the energy harvester. Demori et al. [43] presented a PE-FBEH where a flexure beam was oscillated by von Karman vortices that were dislodged from the upstream bluff body, as depicted in Figure 4a. The ideal positioning of the beam behind the bluff body

has been determined from the simulation findings. During experimental characterization, the electrical output of the harvester was measured for various flow velocities and beam orientations. The system could be improved by extending the operational spectrum and attaining a wider range of optimum velocities. In addition, the bluff body presented here is quite a generic obstacle; the optimization of the bluff body shape can be another consideration within the scope of this work.

Researchers developed unimorph and bimorph piezoelectric cantilever beams [44,45] with different shapes of bluff bodies. Kan et al. [46] implemented changes in the bluff body geometry. The interaction between a downstream diamond-shaped baffle and a cylindrical shell presents a novel way to modify the bluff body's aeroelastic instability. The maximum output voltage increased from 19.8 V to 200 V (by over 900%), offering a viable way to improve the efficiency of conventional VIV-based energy harvesters. Therefore, altering the geometric properties of structures and introducing attachments on the surface of oscillators can increase the output of FBEHs.

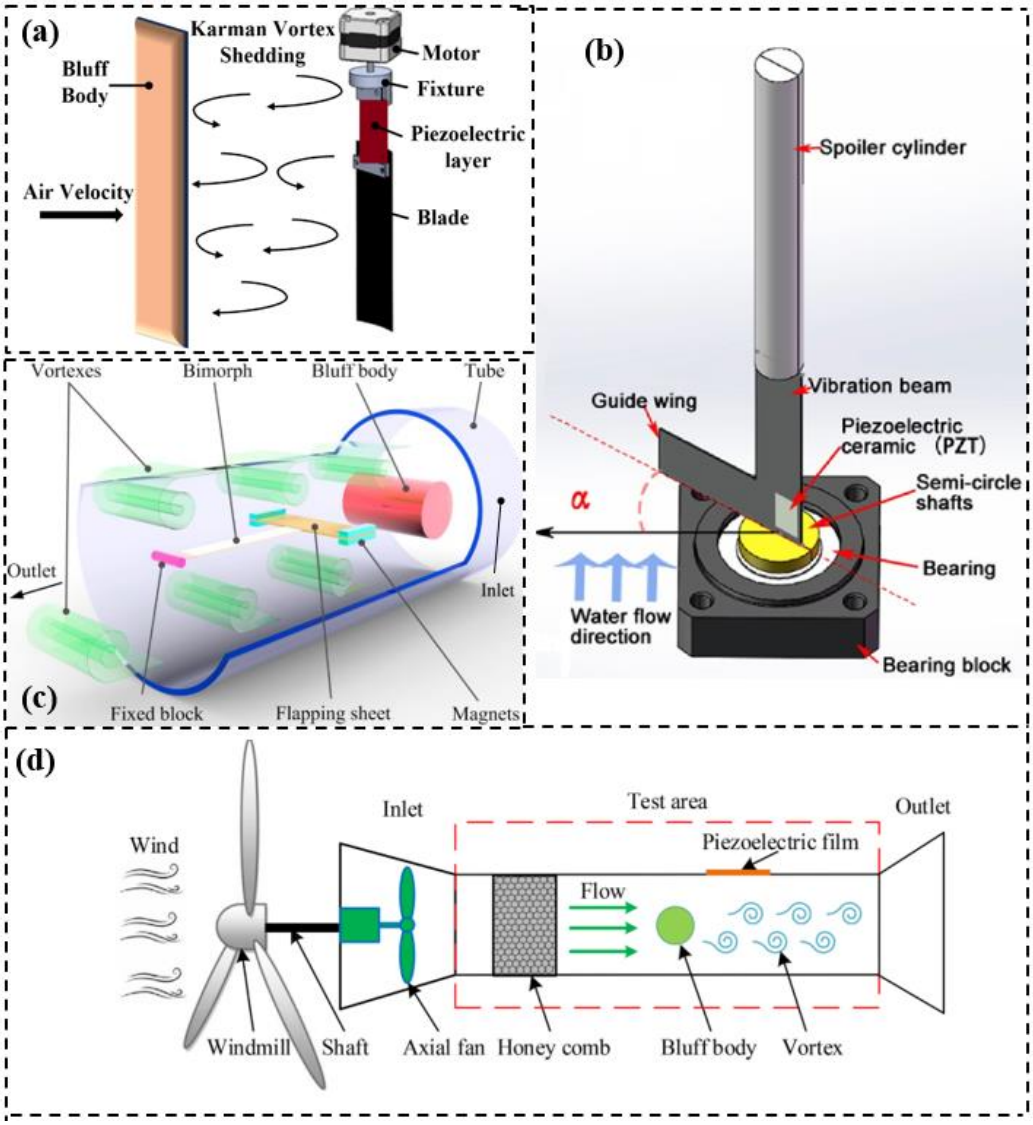

Figure 4. Karman vortex street-based PE-FBEHs. (**a**) Schematic of energy harvesting from von Karman vortices in airflow [43]; (**b**) Direction-adaptive EH with a guide wing reproduced with permission from [47], Elsevier, 2019; (**c**) VIV energy harvester reproduced with permission from [48], Elsevier, 2018; (**d**) Schematic of VIV micro windmill with three blades reproduced with permission from [49], Elsevier, 2022.

The majority of energy harvesting systems prioritize piezoelectric optimization over design performance in real environments with low-density wind energy [49]. To extract wind energy, a micro windmill with three blades (Figure 4d), a circular polyvinylidene difluoride (PVDF) piezoelectric harvester and an air blast blower is set in a wind tunnel. The vortex-induced high-frequency resonance subsequently raises the excitation force amplitudes and enhances the piezoelectric energy harvesting efficiency. However, there is a need to design the energy harvester with strong coupling in the wind field in order to improve the performance at resonance. Another challenge is the power control circuit which can be worked upon as the output power of the reported harvester is comparatively low.

The application of energy harvesting systems has extended to the sea and ocean as natural sources carrying huge quantities of energy [50–52]. Through energy harvesting technology, a tremendous amount of energy can be exploited for either large-scale power grid networks or small-scale dispersed off-grid electronic devices. Such types of large-scale energy harvesting are reported in [47]. The energy harvester in Figure 4b shows the prototype's guiding wings to turn with water flow. The guide-wing technology provides the harvesters with all-around multi-directional sensitivity, which will speed up the adoption of energy harvesters in oceans. Considering the orientation of the tip mass as an important aspect of VIVs energy harvesting, Dai et al. [53] investigated the features of four different vortex-induced PE-FBEHs with emphasis on the effects of the bluff body's orientation on the natural frequency, damping, synchronization region and the output of the harvester. In continuation to achieve effective orientations of bluff bodies, Zhou et al. [54] designed a PE-FBEH to be used in rotational equipment. Their investigation shows that the diameter of the cylindrical obstacle has a less significant impact on the energy harvester's generated power output than the rotation speed and installation angle. Hu et al. [48] studied how shedding-induced forces caused by an oscillating flap sheet interact with a piezoelectric beam as depicted in Figure 4c. According to their lumped parameter model, the distance between the piezoelectric beam and the bluff body was optimized for enhanced energy harvesting. Recently, Wang et al. [55] reported a novel technique of topology optimization in VIV energy harvesters. A topological optimization analysis was performed on the distributions of the two piezoelectric materials. The long, trapezoid shape offered the maximum energy harvesting capacity, depending on the reinforcing material used in the design. When using piezoelectric material as a design variable, the short trapezium model provided maximum output from energy harvesting. It can be concluded that optimizing the distribution of reinforcement/substrate structures should be more important than focusing on the piezoelectric material itself.

3.2. Karman Vortex Street-Based EM-FBEHs

Vortex-induced electromagnetic energy harvesters leverage the principles of electromagnetism to convert FIVs into electrical power. As vortices form and shed behind a bluff body in a fluid flow, the resulting oscillations cause a relative motion between a magnet and a coil. According to Faraday's law of electromagnetic induction, this motion induces an electromotive force (EMF) in the coil, generating electrical current. Wang et al. [56] fabricated an electromagnetic flow-based energy harvester (EM-FBEH), where the pressure variations in fluid flow were applied to a flexible diaphragm with a magnet attached, which was surrounded by a wound coil. As a result, the motion of the magnet with respect to the coil induced EMF in its terminals. Experiments demonstrated that when the excitation pressure oscillated with an amplitude of 254 Pa and a frequency of 30 Hz, an output peak-to-peak voltage of 10.2 mV was produced. Wang et al. [57] reported an EM-FBEH capable of capturing energy from vibrations caused by the Kármán vortex street. The periodic pressure oscillations from the Kármán vortex street in the flow channel cause the magnet beneath a coil to oscillate, generating voltage. The energy harvester prototype of 37.9 cm^3 was tested at an excitation pressure of 0.3 kPa and frequency of 62 Hz, with an output peak-to-peak voltage of about 20 mV achieved. Recently, Sarviha et al. [58] also utilized the diaphragm mechanism to develop a flow-based electromagnetic energy harvester.

3.3. Karman Vortex Street-Based TE-FBEHs

Zhang et al. [59] suggested a VIV-based TE energy harvester (TEEH) that enabled efficient energy harvesting from wind at low speeds. The harvester comprised a cylinder, springs and friction layers, as shown in Figure 5a. The cylinder was attached to springs and a polyaniline friction layer, which allowed it to move up and down. Polytetrafluoroethylene (PTFE) was another friction layer that was fixed at the lower section. With a wind speed of 2.78 m/s, an average power of 392.72 μW and power density of 96.79 mW/m^2 were obtained.

Wang et al. [60] developed a VIV-TEEH, featuring a wind vane along an internal power generation unit, external frame, four springs, square cylinder and circular turntable. The internal power generation unit consisted of PTFE balls, a honeycomb frame and two copper electrodes. Unlike most prior TEEHs, the bouncing PTFE balls were entirely bundled in a square cylinder. The unique design isolated the contact electrification process from the surrounding environment while preventing frictional wear in traditional triboelectric devices.

Li et al. [61] reported a novel design of TEEH based on VIVs that captures the kinetic energy of a low-speed water flow. The harvester was primarily made of a cylinder and a cantilever beam containing two nanogenerator units, as depicted in Figure 5b. The maximum voltage of 174 V occurred at 2 Hz of vortex resonance (flow speed of 0.5 m/s), with a power output of 2.5 mW at 1 MΩ resistance.

Recently, a unique flag-type TEEH with a Y-type bluff body (Figure 5c) has been reported in [62] for harvesting wind energy. The Y-type bluff body amplified the vibration of vortices shedding. The mounting position, design dimension and windward angle of the Y-type bluff body were explored to improve flag vibration and triboelectric power output. At a wind velocity of 6 m/s, the maximum output power was 2.9 μW with 8 MΩ load resistance. A Y-shaped bluff body offers substantial potential for powering numerous sensor nodes across a broad range of wind speeds.

Choi et al. [63] developed a rolling-based TEEH, which can efficiently harvest wind energy from all directions, utilizing a circular guide vane and a deformable rolling cylinder for effective triboelectrification, as shown in Figure 5d. The airfoil-shaped guide vane consistently shed rotating vortices which eventually increased the speed beyond the actual input speed. At 8 m/s wind speed, an RMS voltage of 120 V and RMS power of 1.94 mW at 40 MΩ were achieved.

Table 2 represents the VIV-based energy harvesters discussed above, the output of which ranges from several μW to few mW at different wind speeds. The output generated in [48,54] was higher due to additional elements contributing to the vortex generation and thereby the vibration amplitude of the energy harvester. Additionally, the TEEHs [61,63] produced more output power, mainly due to structural parameters like springs and the shape of the wind vane, increasing the vortices shedding and eventually enhancing the actual wind speed. These features make their use more favorable in varying environments and thereby increase the range at which energy can be collected.

Table 2. Summary of VIV energy harvesters.

Harvester Type	Fluid Velocity (m/s)	Output Voltage (V)	Resistance (kΩ)	Output Power (μW)	References
PE-Turbulence induced vibration	7.125		100	4	Akaydin et al. [41]
PE-Water based	0.35		125	84.49	Song et al. [42]
PE-Airflow based	4		15	1300	Demori et al. [43]
PE-Flapping sheet	2.4	19.2	12	15,300	Hu et al. [48]
PE-Micro windmill	19	5.06	650	8.97	Du et al. [49]
PE-Rotational wind EH	12	10	100	1000	Zhou et al. [54]

Table 2. *Cont.*

Harvester Type	Fluid Velocity (m/s)	Output Voltage (V)	Resistance (kΩ)	Output Power (μW)	References
EM-Water based	1.38	0.02	0.038	1.77	Wang et al. [57]
TE-Wind induced vibration	2.78	536	83,300	392.72	Zhang et al. [59]
TE-Water based	0.5	174	1000	2500	Li et al. [61]
TE-Flag type	6		8000	2.9	Han et al. [62]
TE-Rolling based mechanism	8	120	40,000	1940	Choi et al. [63]

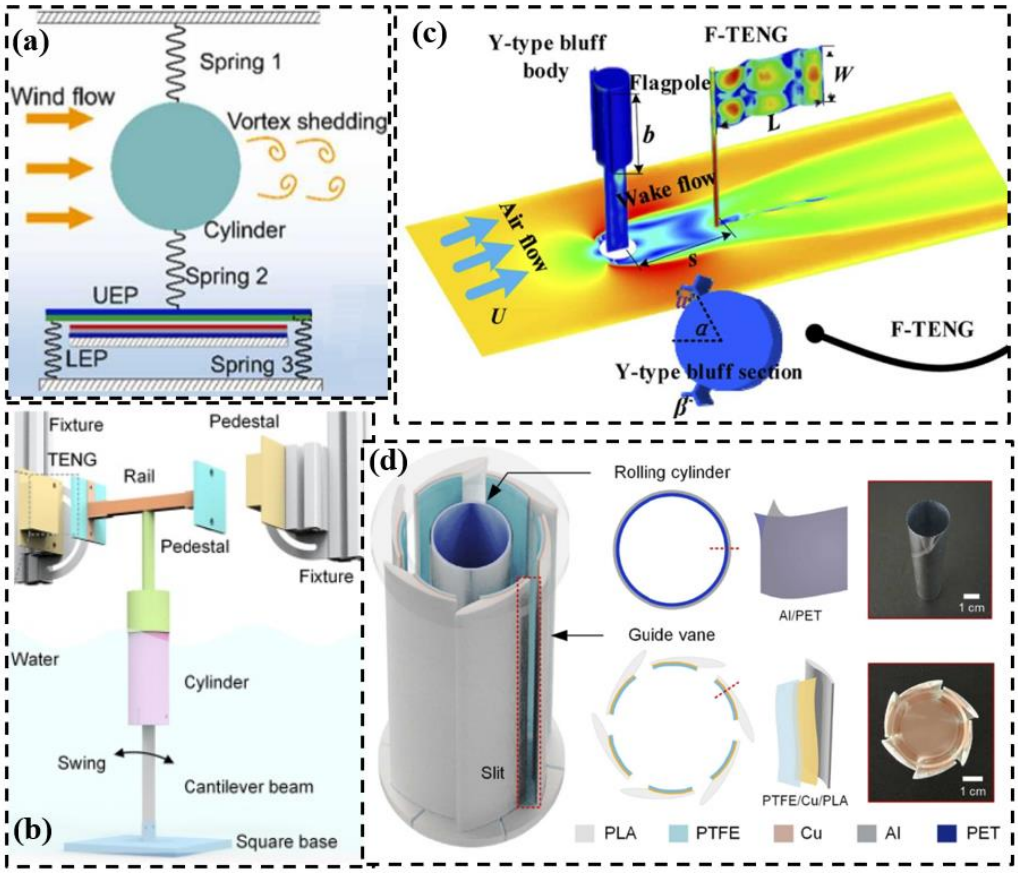

Figure 5. VIV-TEEHs: (**a**) TEEH with springs reproduced with permission from [59] Elsevier, 2022; (**b**) Hydrokinetic TEEH reproduced with permission from [61] Elsevier, 2023; (**c**) Y-shaped/flag-type TEEH reproduced with permission from [62] Elsevier, 2024; (**d**) Vortex-induced rolling TEEH reproduced with permission from [63] Elsevier, 2024.

4. Galloping Energy Harvesting

Galloping is a self-excited vibration phenomenon generated by aeroelastic instability, which occurs in structures with edges and corners usually known as prismatic structures. It is characterized by low-frequency and high-amplitude oscillations. It appears to be related to the velocity of the entering flow and the relative direction of the fluid regarding the structure [64]. When the incoming airflow speed is low, the damping of the system is positive, and the structural vibration will slowly decay to zero. When the incoming airflow speed gradually increases and exceeds a critical value, transverse oscillations perpendicular to the direction of the wind flow in structures (with low damping) occur. When there is further increase in the flow velocity, there will be further decrease in net damping, i.e., negative damping is achieved, which leads to self-excited oscillations also known as Hopf

bifurcations. Limit cycle motion takes place when the structural amplitude becomes stable, and the damping slowly increases from negative to zero. In comparison to VIVs and flutters, structural vibrations are a preferable option for galloping energy harvesting due to their larger vibration amplitude and capacity to oscillate over an infinite range of wind velocities [65]. Typical behavior of a galloping energy harvester in terms of flow velocity and the amplitude of structural vibrations is explained with the help of Figure 6a.

Numerous fundamental investigations were carried out in the early stages of the development of galloping-based energy harvesting devices to gain a thorough understanding of their viability. For the first time, a single-degree-of-freedom model was put forth by Barrero-Gil et al. [26]. In this study, the potential application of transverse galloping in wind energy harvesting was theoretically examined. To further understand the underlying parameters influencing energy harvesting efficiency, a variety of experimental investigations have also been conducted using piezoelectric, electromagnetic and triboelectric transduction mechanisms.

4.1. Galloping PE-FBEHs

Sirohi and Mahadik [66,67] devised a variety of galloping energy harvesters with cantilevers and attached prisms with triangular and D-shaped cross-sections. The impacts of the cross-section geometry of the bluff body on the onset speed of galloping-based piezoelectric energy harvesters (PEHs) were studied theoretically and experimentally by Abdelkefi et al. [68] and Zhao et al. [69]. It was demonstrated that energy harvesters with square-shaped cross-sections operate most effectively. Consequently, many researchers developed energy harvesting systems with improved and unique-shaped bluff bodies [70,71]. Hu et al. [72,73] investigated the installation of rods or fins along the edges of bluff bodies as an aerodynamic modification approach to enhance aerodynamic performance. Liu et al. [74,75] constructed a Y-shaped bluff body and a fork-shaped bluff body (Figure 6c). Wang et al. [76] discovered that the Y-shaped galloping energy harvester performs significantly better than the square-shaped galloping energy harvester. Recently, Sun et al. [77] devised a bulb-like cross-sectional (Figure 6b) bluff body to achieve higher efficiency over a broad operational wind velocity range. To improve the efficiency of a PE-FBEH, Zhou et al. [78] presented a curved-plate bluff body and compared it to bluff bodies with standard cross-sections (square, regular-triangle and D-shaped cross-sections). According to their experimental findings, a curved-plate bluff body with a particular arc length can produce a larger output voltage and a lower cut-in wind velocity. A similar approach of the curved-tip body of a galloping energy harvester was presented by Harvey et al. [79]. Better aerodynamic efficiency is made possible by the blade shape, which is curved, resembling an airfoil rather than a bluff body. Noel et al. [80] attached a rigid splitter structure to the end of a square bluff body. The results indicated a 67% increase in the output power. Jo et al. [81] used a square prism galloping energy harvester surrounded by an enclosure which experiences an increase in aerodynamic force as a result of the movement of the bluff body in relation to the enclosure. Zhao et al. [82] introduced a square cylinder with a V-shaped groove on the windward side that can change both the lateral force on it and the critical velocity (ranging from 2.53 to 4.69 m/s). This approach enhanced the output power by 61%. A similar approach in [83] was also focused on the galloping energy harvester's performance by analyzing the effects of different V-groove depths on the bluff body. The harvester produces its highest output power in environments with low wind speeds. Wang et al. [84] developed a cut-corner prism type PE-FBEH based on a galloping enhancement mechanism, as illustrated in Figure 6d. An innovative, galloping energy harvester in the shape of a funnel was presented by Zhao et al. [85]. It has a high normalized harvesting power and a broad working wind-speed range. The structural non-streamline fluid flow is improved by this topological aerodynamic design, and the pressure direction is made to follow the lift-force direction, increasing the aerodynamic force, and improving the efficiency of the energy harvester. Yuan et al. [86] developed a novel FIVs energy harvester based on a corrugated-shaped bluff body as illustrated in Figure 6e, which was tested at

low wind speeds resulting in a 189% increase in response to a 2 m/s wind speed. In [87], the PE-FBEH utilizing a double bluff body exciter provided great reliability, the ability to generate power at low wind speeds and adaptability to varying wind conditions. Another approach reported by Liu et al. [88] investigated the durability and adaptability of a PEH in variable wind conditions. A double-airfoil-structured bluff body (Figure 6f) with adjustable attack angles is suggested to exploit the advantages of various types of FIVs based on the local wind speed.

Besides the optimization and changing of the geometric characteristics of the bluff bodies, the practicality of wind energy harvesters in real environments is highly anticipated. Tan et al. [89] examined the environmental feasibility of a galloping energy harvester for practical applications across different regions and seasonal changes. Hu et al. [90] investigated how the surface roughness of a bluff body affects the efficiency of the energy harvester. The results of the investigation showed a significant increase in the piezoelectric energy harvester's environmental adaptability, preventing fatigue damage or even cantilever beam breakage at higher water velocities caused by the occurrence of excessive vibrations. To enhance the effectiveness of galloping wind energy harvesters in natural and unpredictable environmental conditions, Xia et al. [91] proposed a PE galloping energy harvester featuring a tri-section beam with piezoelectric transducers and a square bluff body with splitter attachments, as shown in Figure 6g. A finite element analysis confirmed the clustered natural frequencies for multi-mode excitation. This confirms the harvester capturing wind energy across a wide range of incident directions by exciting multiple modes. Optimal performance was achieved when the second bending mode was activated. The novel design offers a promising solution for harvesting wind energy in varying natural conditions.

4.2. Galloping EM-FBEHs

Converting ambient and aeroelastic vibrations to useable electrical energy with galloping EM-FBEHs has also been in use for operating low-power electronic devices. In [92], a theoretical model was generated and experimentally verified by utilizing three different cross-sections (square, triangular and D-shaped) of the bluff bodies. A was magnet attached to a beam vibrating with respect to a stationary coil. It was observed that maximum power of 37 μW was obtained at a wind speed of 3.25 m/s and load resistance of 300 Ω when using the D-shaped bluff body. Zhang et al. [93] developed a Y-shaped bluff body as shown in Figure 7a. The bluff body's aeroelastic response caused the coil to cut the magnetic induction lines. An average power of 2.5 mW was measured at 4 m/s wind speed with the Halbach effect, which is superior to other aeroelastic energy harvesters reported in the literature. Moreover, it is also more environmentally adaptable.

Recently, Xiong et al. [94] proposed a spring-coupling (Figure 7b) galloping EM-FBEH to enhance the output characteristics in a high-speed flow field. The coupling spring's stiffness and the initial gap between it and the bluff body will have an impact on the output characteristics. The output power was up by 92.7% when compared with the energy harvester without a coupling spring.

Most of the research on energy harvesters concentrates on transverse galloping. The term "torsional galloping", which refers to a back-and-forth rotation of the bluff body, is effective in confined places and can also be integrated with the energy harvesters. Additionally, adding extensions to it gives a boost to torsional galloping-based EHs. The study in [95] focused on torsional galloping EM-FBEH. Figure 7c (i) shows the schematic of the initial prototype, featuring a bluff body connected to the DC generator. Figure 7c (ii) illustrates the modified design of the torsional EH, which integrates three beams and linear springs. The modified design helps bluff body to exhibit a combinations of transverse and twisting modes, which marks its suitability for the development of self-sustained environmental sensing systems.

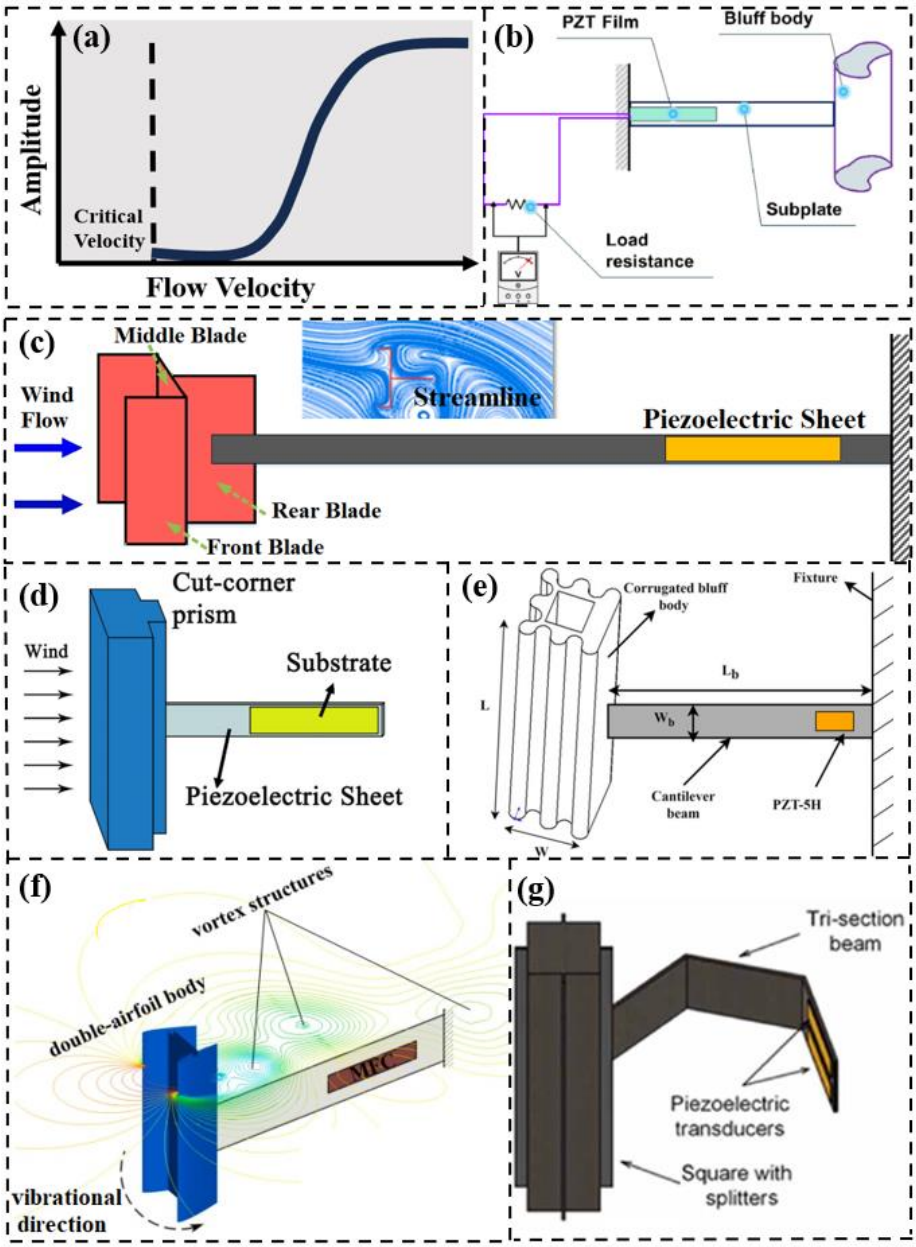

Figure 6. (**a**) Typical trend of a galloping flow energy harvester; galloping-based PE-FBEHs with different shaped bluff bodies: (**b**) bulb-like cross-sectional reproduced with permission from [77] Elsevier, 2019; (**c**) fork-shaped reproduced with permission from [75] Elsevier, 2019; (**d**) cut-corner prism reproduced with permission from [84] Elsevier, 2021; (**e**) hyper-structure corrugated [86]; (**f**) double-airfoil reproduced with permission from [88] Elsevier, 2023; (**g**) tri-section beam and square body with splitters [91].

Su et al. [96] developed a novel EM-FBEH that uses parallel elastic strips suspended in a hollow square tube with magnets, as shown in Figure 7d. When the wind velocity increased to 4 m/s, the average power was 7.8 mW, with an RMS voltage of 3.2 V produced at an optimum resistance of 1.2 kΩ.

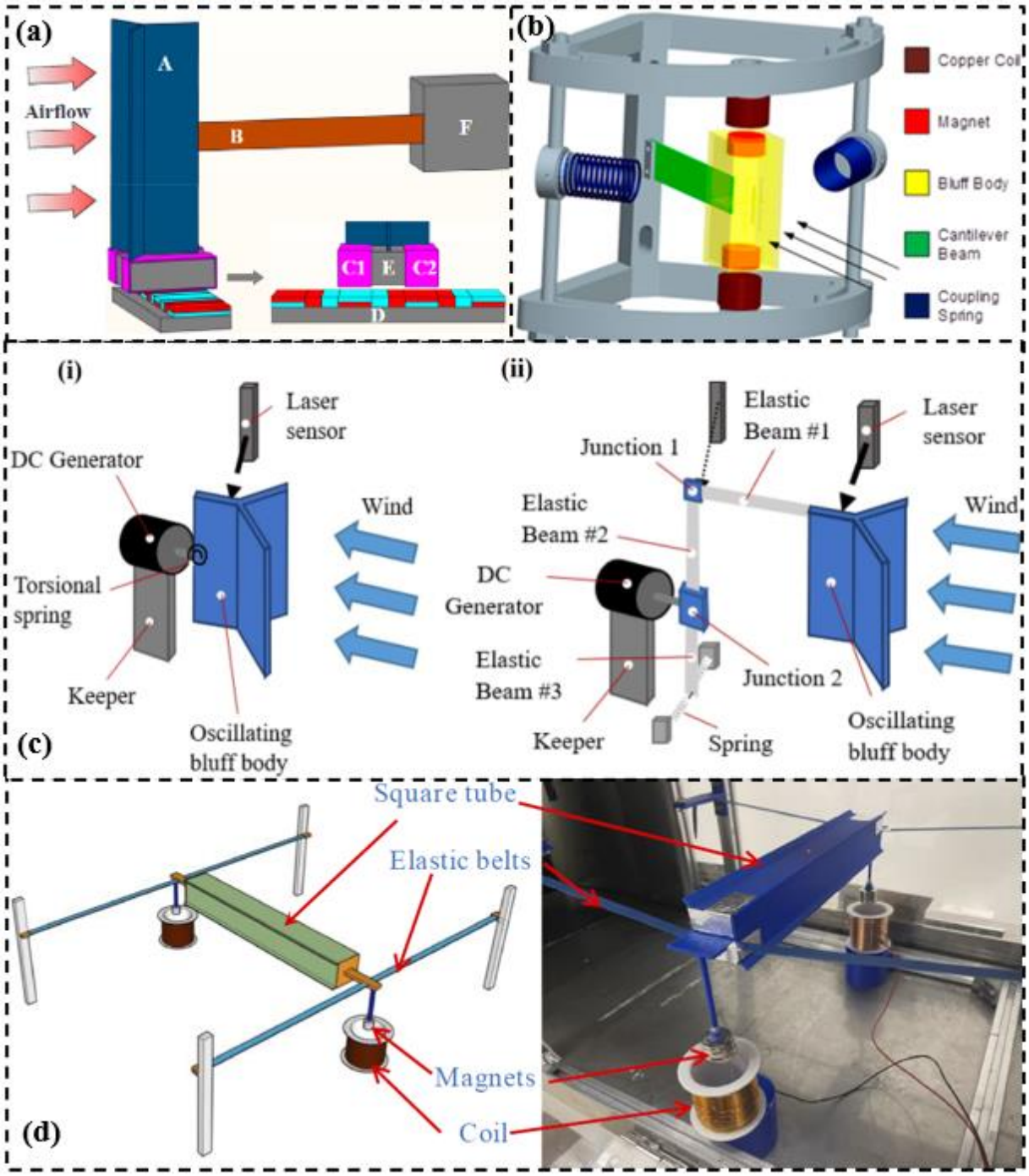

Figure 7. Galloping EM-FBEHs: (**a**) Halbach effect EH reproduced with permission from [93] Elsevier, 2019; (**b**) spring-coupling EH [94]; (**c**) (i) torsional galloping EH, (ii) modified design with beam elements reproduced with permission from [95] Elsevier, 2023; (**d**) elastic strips suspended EH reproduced with permission from [96] Elsevier, 2024.

4.3. Galloping TE-FBEHs

When an elastic structure is exposed to fluid flow, the transverse oscillations from galloping can be converted into friction and separation processes in TEEHs. The impact behavior due to galloping was presented in [97]. The harvester can generate over 200 V at wind speeds as low as 1.4 m/s. This work marks the restriction of onset wind speeds in TEEHs. However, TEEHs still face a number of obstacles in the collection of low-speed wind energy, including significant energy loss and damaging friction wear. Zeng et al. [98]

developed a novel TEEH based on galloping to address these issues. The TE components of the energy harvester were bundled in a bluff body to prevent environmental disturbances, eliminating the significant rotation resistance and frictional wear found in conventional designs. A TEEH inspired by fish fins was reported in [99]. The beam structure with soft materials swayed in the water flow, causing the small sphere within the bluff body to produce electrical impulses via surface friction. The energy harvester had an open-circuit voltage ranging from 200 V to 313 V at flow velocities of 0.24 to 0.89 m/s. Remarkably, even after 30 days of immersion in water, the output of the device stayed at 96.81% of its original value. This resilience to water immersion demonstrates the device's endurance, as well as its potential for long-term energy harvesting in aquatic or underwater environments.

Cao et al. [100] introduced a unique technique for parametric optimization and large-scale standard and customized manufacturing of TEEHs. The TEEHs were combined with a wind-induced galloping oscillator to gather omnidirectional wind energy. The design included a Y-shaped mast with a magnetic tuning system, providing a strong reaction to breeze while maintaining system resilience. Beyond wind energy, the adaptable energy packs can be used as ocean waves or human motion harvesters in network setups, powering a vast real-time monitoring sensor array.

Several galloping energy harvesters reported are summarized in Table 3. The comparison was performed on the basis of cut-in velocity, shape of the bluff body or modifications in the bluff body and output power generated by the energy harvesters. The optimum resistance and the velocity at which the maximum power is generated play an important role in the efficiency of the energy harvester, whereas the choice between PE and EM depends on the frequency characteristics of the FIVs. Due to their greater power-generating capabilities at low frequencies, PE harvesters thrive in low-frequency applications. The research works [86,87] show their ability to generate power at low wind speeds and adaptability to varying wind conditions. EM harvesters, on the other hand, are better suited for high-frequency applications. The topological design as well as the angle of attack both have a considerable impact on the aerodynamic properties. As the aerodynamic forces increase, the efficiency of the EH improves, as seen in [88]. However, the durability, practicality and resistance to harsh environments are concerning. The work conducted in [90] well explains how varying the geometric properties achieves better performance and robustness in challenging conditions. Likewise, the change in geometric properties, i.e., in bluff bodies, contributes to lowering the threshold wind speeds and achieving a broad working range. This can be clearly seen in Table 3, where the cut-in speed for each bluff body configuration is highlighted. The TEEH in [97] has excellent geometric characteristics generating a high voltage at a very low wind speed, whereas [98] focuses on parametric optimization leading to system resilience and efficiency to capture energy in multi-directions. It has a slightly higher cut-in speed and compared with the rest of TEEHs mentioned, it has a higher output. This design also tackled issues with the existing wind energy harvesters based on TEEHs, such as poor stability, short lifespan and high wind-speed requirements. Likewise, in [99], the cut-in speed was drastically reduced to adapt to low velocity water flow for energy aligning with natural rhythms.

Table 3. Galloping FEHs.

Shape of the Bluff Body	Cut-in Velocity (m/s)	Optimum Resistance (kΩ)	Velocity at Max Power (m/s)	Voltage (V)	Output Power (mW)	References
PE-FEHs						
Square	2.5	105	8		8.4	Yang et al. [65]
Square with fins		5000	5		0.034	Hu et al. [72]
Y-shape	1	1000	5	40	1.6	Liu et al. [74]
Fork-shape	1.5	1000	5	32	1.07	Liu et al. [75]

Table 3. *Cont.*

Shape of the Bluff Body	Cut-in Velocity (m/s)	Optimum Resistance (kΩ)	Velocity at Max Power (m/s)	Voltage (V)	Output Power (mW)	References
PE-FEHs						
Y-shape	1.32	2006	2.098		1.19	Wang et al. [76]
Curved plate	1.8	820	5.5	10.7	0.0356	Zhou et al. [78]
Splitter plate	3	0.593	7		14.8	Noel et al. [80]
Square	1.9	2730	4		0.018	Jo et al. [81]
Square with V-shaped grooves	3.04	9	10		0.93	Zhao et al. [82]
Square with V-shaped grooves	1.75	180	9		15.24	Siriyothai et al. [83]
Cut-corner prism	3.8	100	6.24		47.5	Want et al. [84]
Funnel shape	7	300	24		4.3	Zhao et al. [85]
Hyper-structure corrugated	3		6	0.89	31.3	Yuan et al. [86]
Double bluff body	0.96	2000	15	90.35	2.57	Wang et al. [87]
Double-airfoil	1.5	411.2	8	163.39	26.67	Liu et al. [88]
Elliptical	0.3	4000	0.55	38.4	4.2	Hu et al. [90]
EM-FEHs						
D-shape	-	0.3	3.25	0.105	0.037	Ali et al. [92]
Y-shape	1.5	0.3	4	1.4	2.5	Zhang et al. [93]
Square	3	-	14	0.103	0.79	Xiong et al. [94]
Y-shape	2.75	0.044	10	0.118	0.31	Kim et al. [95]
Hollow square tube	1.6	1.2	4	3.2	7.8	Su et al. [96]
TE-FEHs						
Y-shape	1.4	50,000	6	200	0.01	Zhang et al. [97]
Trapezoid	2.9	44,000	7.8	-	1.3	Zeng et al. [98]
Fishtail-shaped	0.24	-	0.89	313	-	Zhang et al. [99]

5. Flutter Energy Harvesting

Flutter is a type of self-excited motion, which occurs owing to coupling between the aerodynamics and the structure. The flutter motion is related to the bending and torsional vibration of the structure, which usually occurs at high wind-speeds. When the environmental wind speed exceeds a critical value, the structure starts to vibrate with a large amplitude [101]. Just like galloping, the flutter phenomenon results from negative damping. Unlike galloping, it typically occurs in structures with a sheet-like shape (such as flat plates, membranes, wing-shaped structures, etc.) and flutters frequently with a chaotic aerodynamic force [102]. Due to system nonlinearities like geometric nonlinearity caused by substantial deformation, structural gaps and nonlinear aerodynamic behavior due to high angle of attack, the increasing amplitude is constrained practically. As a result, the system attains limit cycle oscillation (LCO). Due to the self-excitation and large amplitudes of vibration induced by flutter, the flutter-based energy harvester offers a great deal of scope for advancement in terms of energy harvesting [103]. Owing to its efficiency, compact size and flexibility, piezoelectric flutter FEHs dominate the literature, in comparison with electromagnetic flutter FEHs in most research and practical applications.

5.1. Flutter PE-FBEHs

In 2008, a morphing airfoil was employed by Erturk et al. [104] to capture aeroelastic energy from airflow. Since then, a wide range of energy harvesters have been developed and investigated. For instance, Erturk et al. [105] proposed the idea of using aeroelastic flutter to harvest wind energy. Numerical simulation and experimentation was performed, and the impact of flutter velocity on piezoelectric energy harvesting was examined. Bryant et al. [106] developed a semi-empirical unstable aerodynamic model to simulate and analyze the stall behavior of the structure. In [107], a T-shaped PE-FBEH operated on the principle of aeroelastic flutter, which occurs at low fluid speeds. It was found that a harvester of size 1006 cm^3 could provide 4.0 mW of power at a wind speed of 4 m/s. The maximum speed to allow safe operation was not identified (it was tested up to 15 m/s), so the device maximum output was not concluded. Moreover, there was no clear evidence of the onset flutter speed, hence the frequency range was not defined. To enhance the performance of a flutter-based energy harvester, it was integrated with an airfoil as shown in [108]. The device was proven to function better under the combined loading, wind and base excitations in terms of its transduction abilities, and power density even while operating below its optimum speed. Experimentally, a 150% increase in output power per unit acceleration was observed when the wind speed was increased from 0 to 2 m/s, which was below the flutter speed of 2.3 m/s. However, the reported model does not account for adaptability in the real environment, and also, a prediction of the harvester response in terms of stability potentials was not performed.

In [109], a stepper motor connected to the composite beam was controlled to set the static angle at the base of the beam. The experiments were performed at several angles. At a flow speed of 9 m/s and 7.2° angle, a maximum output of 0.272 mW was achieved. Such types of airflow energy harvesting from flutter are widely used in providing power to autonomous sensors in applications like building management systems. Eugeni et al. [110] investigated flag-flutter-based energy harvesting via piezoelectric transduction using numerical analysis and experimentation. Furthermore, the flutter instability of a cantilevered flag with piezoelectric (PZT) and Aluminum (Al) patches was explored. For a 66.6 kΩ resistance, the highest power output produced was 1.12 mW during the experiments. Ankit and Ashish studied the dynamics of a planar structure's flutter oscillation in the presence of an additional wake field with the goal of enhancing the efficiency of a flutter-based energy harvester [111]. The output of 1.46 V and 6.81 µW were obtained at a critical flutter velocity of 6.6 m/s. The study in [112] also sought to improve the understanding of bluff bodies; optimization parameters and piezoelectric flags, as shown in Figure 8, were used. Various rigid cylindrical shapes were placed upstream in the airflow. The results showed that adjusting the stiffness of the flag resulted in a significant increase in power generation. Notably, the highest power output of 746 µW and 19.31 V (RMS) was achieved when the 120° bluff body was coupled with a stiff, short flag.

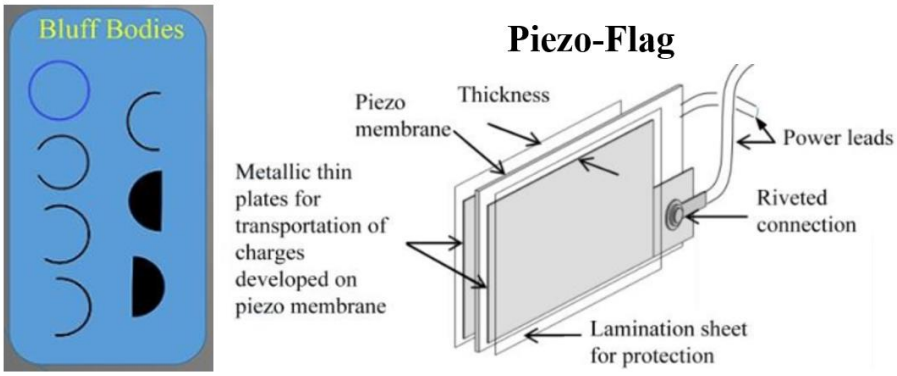

Figure 8. Piezoelectric flag tested with various bluff bodies reproduced with permission from [112] Elsevier, 2023.

5.2. Flutter EM-FBEHs

Zhu et al. [113] described a flutter-based EM-FBEH, using an airfoil linked to a cantilever beam which bends due to airflow over the airfoil. The beam's bending depends on the lift force from the airfoil and the beam stiffness. Figure 9a illustrates a permanent magnet linked to the airfoil and a coil attached to the harvester's base. The magnetic flux cutting the coil changes as the airfoil moves, resulting in the generation of electrical power. At wind speeds as low as 2.5 m/s and 5 m/s, the harvester output was 470 μW and 1.6 mW, respectively. An EM-FBEH [114] was utilized to capture energy from the self-excited aerodynamic response of a T-shaped cantilever structure. The T-shaped cantilever, which had a vertical plate attached to the windward side of a horizontal plate, produced large vortex patterns at its leading edge. These vortices generated considerable lift as they traveled downstream, generating rotational instability at low wind speeds due to interactions between the upper and lower surfaces. Mechanical and electrical damping parameters were employed in the harvester to determine the ideal load resistance and the critical wind speed at which fluttering occurred. The harvester generated 1.1 mW of average power at 8 m/s. Quy et al. [115] investigated the effects of performance design factors such as wind speed, the position and size of the magnets, the pre-applied tension of the membrane, the angle of attack of the membrane and the orientation of the harvester in the flow field. The model shown in Figure 9b consists of a flexible membrane, coil, magnet and support. Experiments demonstrated that a single wind belt can provide power from 3 to 5 mW. Moreover, it is observed that the wind panel generates power of about 50 mW at a wind speed of 7 m/s. A wind panel made up of five such wind belts can produce power between 30 and 100 mW with winds less than 8 m/s. The use of the Karman vortex in belt fluttering EMEH was proposed in [116]. A cylinder was used for the formation of the Karman vortex behind it to induce vibrations when placed in the fluid flow. The membrane strip experiences pressure from the fluid flow, which in turn deforms the belt, and the magnet attached to it oscillates due to which the coil experiences a changing magnetic flux density and hence induces electric charge in the coil terminals. The coil voltage of 6 V peak-to-peak was generated at a wind speed of 3 m/s. Lu et al. [117] presented a wind belt-type EM-FBEH with a reduced critical wind speed by positioning the magnets close to the membrane's center. At a wind speed of 10 m/s, the harvester was found to yield a maximum average power of 705 μW.

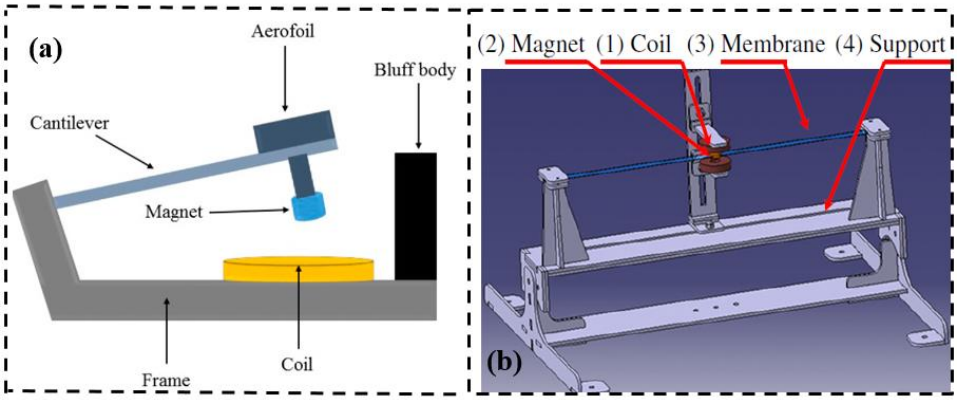

Figure 9. Flutter EM-FBEHs. (**a**) Cantilever-based EMEH [118]. (**b**) Design of wind belt EMEH reproduced with permission from [115] Elsevier, 2016.

5.3. Flutter-Based TEEHs

Triboelectric energy harvesters utilizing flutter provide a novel technique to harvest energy from ambient air flows. The performance of flutter-based harvesters is influenced by the wind direction and variations in airflow patterns. Zhao et al. [119] reported a freestanding, lightweight woven TEEH (W-TEEH) that can capture wind energy from arbitrary directions. The interlaced interactions between Kapton film and a conductive fabric under wind-induced

flapping of the flag ensures the functioning of the W-TEEH flag. This combined contact electrification and electrostatic induction effect work together to generate current. At a wind speed of 22 m/s, about 40 V and 30 μA were the maximum open circuit voltage and current produced, respectively. At a resistance of 6.5 MΩ, the output peak power density reached a maximum of 135 mW/kg. Broadband airflow energy captured using TEEHs operated by aerodynamic flutter was reported in [120]. The thin, free-standing Al foil electrodes that constituted the flutter membrane's unit component were covered on both sides with electrospun poly (vinyl chloride) nanofiber-structured mats, which offered useful tribo-surfaces designed to increase the friction area. Under mild airflow, a single flutter-membrane-based TEEH could generate up to 0.33 μW of triboelectric power. Liu et al. [121] utilized the polarization of a ferroelectric BaTiO3 material in their developed TEEH. A maximum output power of 67 mW was possible with a load resistance of 18 MΩ at a 14 m/s wind speed.

Although flutter-based TEEHs have potential for use with self-powered devices, practically all the described devices are based on parallel structures, which have the flaw of having insufficient triboelectric surface contact. In [122], an angle-shaped TEEH was introduced to solve this issue. A fluorinated ethylene propylene (FEP) film was sandwiched between two Al layers that had been layered to form an angle and were connected on one side to create the device. For the purposes of contact electrification and electrostatic induction, the FEP film could closely contact the Al layers. At an optimum resistance of 4 MΩ, the peak power obtained was 0.82 mW (equivalent to a power density of 26 mW/m^2) when the flow velocity was 25 m/s. This research could provide a substantial and important solution for natural weak wind energy harvesting in practical applications. In [123], a leaf-TEEH was developed using fresh leaves, live leaves, dry leaves, and leaf powders as frictional materials to capture wind and contact mechanical energy from nature. All these leaves were inexpensive and environmentally friendly. The authors used fresh leaves and dried leaves that had fallen as the frictional materials of the harvester for energy harvesting in a green way in nature, which could power an electronic watch and several LEDs when the wind speed was 7 m/s. A maximum power of 17.9 mW was obtained at a load resistance of 11 MΩ.

A wind actuated venturi TEEH [124] transforms ambient energy to produce a periodic vibration of a flag film. A low-pressure zone in the throat region of the venturi system causes the flag film to flutter at high frequencies between the electrodes when air travels through it. By displacing the charge between the electrodes, this flag flapping results in a faster charge transfer efficiency. This charge movement causes variation in the electrode potential which enhances the triboelectrification process. The harvester can deliver an optimum RMS power of 1.5 mW with maximum output power density of 2850 mW/m^2. The study in [125] proposed a flag-type TEEH that is humidity resistant and multi-directional to harvest wind energy and also measure the wind speed. The device was optimized and exhibited higher power generation when bending stiffness and mass ratio were decreased. It was capable of efficiently harvesting wind energy from multiple directions. When two TEEHs are deployed with a gap between them, the wind direction changes and causes them to collide, increasing power density by 40 times. Moreover, the device also worked efficiently in humid conditions, indicating its potential in natural and varying environmental conditions. Recently, Gao et al. [126] integrated a rotating and flutter-induced TEEH for wind energy harvesting and multi-directional wind sensing. The device was optimized to harvest a power of 3.9 mW and was equipped with an eight-channel signal acquisition system to obtain the multi-directional wind vector information in response to wind speeds from 2.6 to 13.5 m/s. The study demonstrated the ability to monitor temperature, humidity, wind speed, and wind direction and detect anomalous vibrations in the wires in real time.

5.4. Bio-Inspired Flutter FBEHs

The application of FIVs is extended to natural environments. Nature provides several sources of FIVs, e.g., fluttering grass leaves or dancing tree leaves are interesting vibrating structures. Several leaf flutter theories [127] and bio-inspired structures [128,129] utilized in wind energy harvesting in the literature are reported.

Li et al. [128] investigated a unique cross-flow stalk configuration for energy harvesting, which differs from standard fluttering devices positioned parallel to the flow direction. The cross-flow stalk arrangement with flexible piezoelectric stalks positioned perpendicular to the flow amplifies vibrations by an order of magnitude, considerably increasing energy extraction. The device was made of low-cost organic piezomaterials for the stalks and polymer films for the leaves and used aerodynamic forces to maximize oscillations, making it suited for cost-effective applications. In addition to leaf-inspired designs, nature's diverse mechanisms for motion extend beyond flora to the intricate wing motions of birds and insects, which offer equally valuable insights for energy harvesting applications. Figure 10a illustrates a TEEH that was inspired by the design and movement of hummingbird wings, intended for efficient and small-scale flutter-based energy harvesting, as reported in [130]. The fluttering mechanism within the wing structure creates movement that leads to contact-separation and free-standing electrification between different triboelectric materials. The device is lightweight (10 g), making it one of the lightest TENGs ever created. This bio-inspired design allows the device to operate effectively under low-frequency wind conditions, even in harsh environments. Inspired by the fluttering mechanics of dipteran insects (such as flies), a bionic multi-domain energy harvester was developed [131]. The wing structures allow for agile flight through rapid flapping motions. The harvester utilizes a flexible cantilever beam that simulates the wings of dipteran insects. This beam can bend and vibrate when subjected to wind or other forces, mimicking the fluttering motion of insect wings. However, it did not account for the output in response to wind energy; vibration energy was used to drive the harvester.

The research in [132] aimed to produce energy from the motion of a branch of a palm tree. The branch was positioned in a wind tunnel and forced to vibrate at an airflow speed of 7 m/s and at an optimum load of 1 MΩ; a maximum power output of 0.157 mW was generated, which corresponded to a power density of 393 mW/m^2. The vertical stalk–leaf arrangement was used by Liu et al. [133] to create a macro fiber composite (MFC)-based flutter energy harvester, as shown in Figure 10b. Wang et al. [134] introduced the inclined angle into the stalk–leaf system. The authors recently developed a bio-inspired architecture of a PEH that has a low cut-in wind speed and constant output frequency [135]. The process of leaf flutter was comprehended by including aeroelastic modeling and laboratory testing of palm leaves. A fake leaf FEH was tested in a wind tunnel at 2 m/s wind speed and at a stable frequency of 3.56 Hz, and an output power density of 1.238 $\mu W/cm^3$ was obtained by the harvester.

Table 4 summarizes and compares several flutter-based energy harvesters, indicating a higher output generation of EM and TE energy harvesters compared with PEHs. Fluttering is a divergent phenomenon, and for larger deflections during fluttering, utilizing EMEHs is a better option. However, the research in [112] focuses on the optimal configurations of the PEH. Optimizing the stiffness of the flag considering the role of structural dynamics in terms of bluff bodies notably increases the power generation. In comparison, the EMEH in [115] considers essential factors such as wind speed, magnet positioning, angle of attack and harvester orientation of the wind flow. All these factors contribute to enhanced output power. Nevertheless, flutter-based TEEHs have more advantages of providing a higher voltage and especially a smaller harvester's volume. Rapid voltage generation and current pulses suitable for triggering alternating-polarity voltage pulses in ferroelectric materials were observed in [121]. This design offers a very high output, small volume and high level of electrical polarization which is necessary for generating the voltage needed for certain applications, such as small-scale high-voltage polarization equipment. Moreover, the effective modulation of output pulses under varying wind speeds showcases its adaptability and control in polarization processes. New materials for TE energy harvesting can assist in natural micro- to nanostructures with high outputs [123], promising environmentally friendly energy harvesting solutions on a large scale. The work carried out in [126] effectively shows a comprehensive approach to capturing wind energy and sensing wind direction, suggesting the promising potential of multi-directional wind sensing to monitor

vibrations generated in transmission lines with considerable outputs to ensure sustainable power sources in designing IoT systems for environmental monitoring.

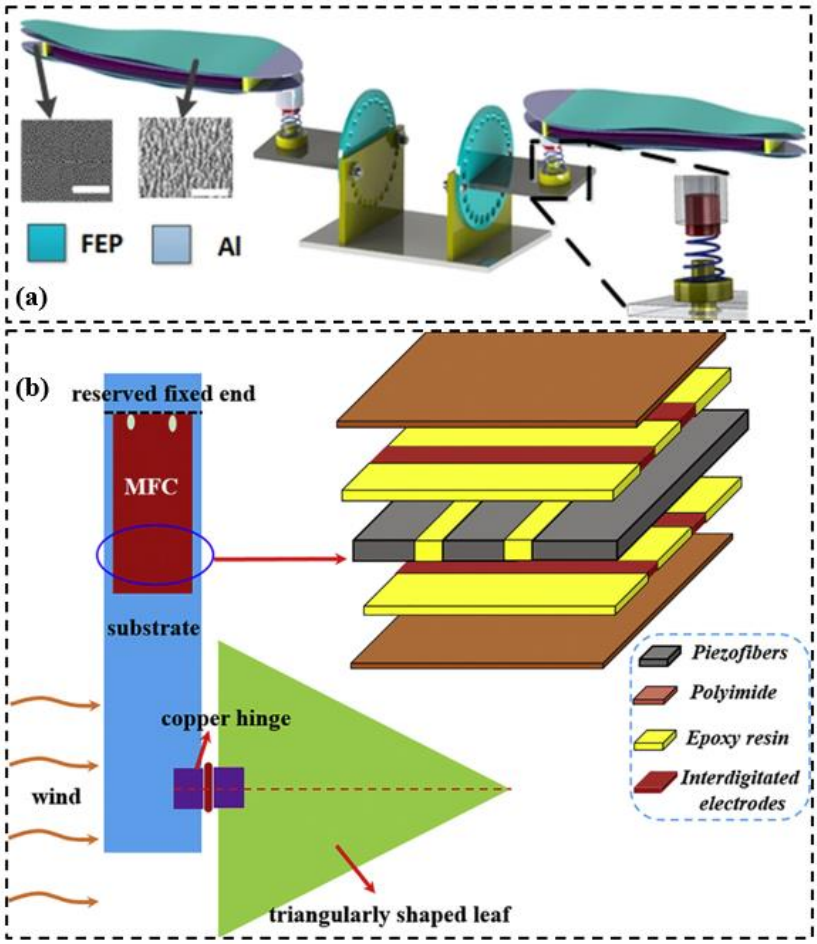

Figure 10. Bio-inspired FEHs: (**a**) wing-stimulated TEEH [130]; (**b**) PEH with MFC layers reproduced with permission from [133] Elsevier, 2020.

Table 4. Summary of flutter-based FEHs.

Fluttering Mechanism	Cut-in Velocity (m/s)	Optimum Resistance (kΩ)	Velocity at Max Power (m/s)	Output Power (mW)	References
PE-FEHs					
Flag flutter	-	66.6	25	1.12	Eugeni et al. [110]
Additional wake	6.6	39	10.6	0.00681	Agarwal et al. [111]
Flag flutter	5	500	20	0.746	Latif et al. [112]
Leaf flutter	-	1000	7	0.157	Al-Haik et al. [132]
-		680	7.5	0.54	Liu et al. [133]
Leaf flutter	2	220	3	0.00076	Wang et al. [135]
EM-FEHs					
Cantilever spring	2.5	4.7	5	1.6	Zhu et al. [113]
-	4	-	8	1.1	Park et al. [114]
Wind belt-type	3	-	7	50	Quy et al. [115]
Wind belt-type	3	0.6	10	0.705	Lu et al. [117]

Table 4. *Cont.*

Fluttering Mechanism	Cut-in Velocity (m/s)	Optimum Resistance (kΩ)	Velocity at Max Power (m/s)	Output Power (mW)	References
TE-FEHs					
Flag-type		6500	22	135 mW/kg	Zhao et al. [119]
Multi-layered membrane		7000	4	0.00033	Phan et al. [120]
Flapping-type		18,000	14	67	Liu et al. [121]
Parallel-structured		4000	25	0.82	Lin et al. [122]
Leaf-flutter		11,000	7	17.9	Feng et al. [123]
Flag-type	0.5	198,000		4.5	Ravichandran et al. [124]
Flag-type		5000	7.5	0.03672	Wang et al. [125]
Rotary-flapping type		9000	10	3.9	Gao et al. [126]
Wing flutter		10,000	7.5	1.5 W/m^2	Ahmed et al. [130]

6. Wake Galloping Energy Harvesters

Wake galloping refers to the diverging oscillations of the downstream bluff body triggered by the wake that originates from the upstream bluff body. The galloping phenomenon is the term used to describe the vibration that occurs when a single cylinder with a flexible base is placed in the wind. However, when an obstacle with a fixed foundation is positioned upstream of the energy harvester, the vortices shed from the upstream obstacle reattach to the downstream body (i.e., the energy harvester). As denoted in Figure 11a [136], the oscillations in wake galloping are created by the wind flow interaction with the structure's wake. The region that consists of disturbed air behind the structure is known as the wake. The wake may become unstable when the wind flow is strong enough. Large-scale vortices may develop in the wake because of this instability. The structure oscillates due to the interaction with these vortices. Wake galloping has its features in that of VIVs, however, there is a slight difference in the position of the oscillating body in relation to the vortex shedding. In fact, for wake galloping, the oscillating body is positioned downstream of an obstacle. As a result, the body oscillates as it interacts with the vortices that the obstacle is shedding. Lock-in or synchronization takes place when the vortex shedding frequency approaches the oscillator's natural frequency, as shown in Figure 11b. Large amplitude motions are produced in this region when flow relates to the oscillator's natural modes of vibration. When the vibration frequency is a multiple or submultiple of the shedding frequency, synchronization can also happen, though to a lower extent. On the other hand, in VIVs, the body oscillates due to the alternate lift forces brought on by the vortices that are shed from its trailing edge.

Zhang et al. [137] numerically investigated two bluff bodies working in tandem. Based on previous studies, for example, Sun et al. [138] and Usman et al. [139], the authors utilized interference cylinders for energy harvesting from VIVs, and the wake galloping phenomenon emerged as an efficient method to harvest energy in a wide range of wind speeds. A PEH was developed by Akaydin et al. [140] by positioning an elastic beam behind a bluff body at a specific distance. Due to the wake created by the bluff body, the structure consequently vibrated, generating a maximum power of 4 μW. Jung et al. [141] experimentally found that the EM-FBEH can produce 370 mW of power under a wind speed of 4.5 m/s at a natural frequency of 4.8 Hz. Sivadas et al. [142] evaluated a number of crucial parameters to optimize the setup of PEHs using the analysis in COMSOL. A flexible beam was installed behind bluff bodies of various shapes in their computational model. According to the results, the cylindrical bluff body produced the highest average power of 0.35 mW. The study in [143] demonstrated the vibration behavior of the tip body (downstream cylinder) affixed to a cylindrical shaped bluff body through a cantilever beam.

The wind flow allowed both transverse and translational vibrations of the tip body. The outcomes demonstrated that the triangle tip body produces the optimum result from a wake-induced vibration energy harvester.

Zhang et al. [144] utilized several cross-sectional interference cylinders illustrated in Figure 11c to boost the energy harnessing performance. For the PEH with a square prism, it generated a peak average power of up to 803.4 μW at 2.36 m/s with a spacing ratio of L/D = 0.9. When compared with the energy harvester without the interference cylinder, the corresponding synchronization region was considerably boosted by 380%. Alhadidi et al. [136] verified that the steady-state bandwidth of wake galloping FEHs can be widened using a bistable restoring force, which reduces their sensitivity to changes in flow speed. A PE-FBEH was reported by Muhammad Usman [139]. For both the upstream and the downstream cylinders, circular cross-sections of similar diameters were considered. At a 10 m/s wind speed and the maximum voltage obtained was 38 mV. Shan et al. [145] presented a double PE-FBEH system in water. The distance between two PEHs, the specific gravity, and the cylinder diameter were all performance variables, whereas the other factors were kept constant. Water traveled from left to right through the first PEH (leading) and the second PEH (following), causing both to vibrate vertically. When the spacing distance between the energy harvesters is large enough, the vortex will cause the beams to vibrate independently. When the spacing is kept small, a coupled vibration between the two energy harvesters occurs. Furthermore, the motion of the following PEH will be affected by the wake created by the leading PEH. The existence of the following PEH, on the other hand, will alter the path of the leading PEH. In this way, the performance of a double PEH is considerably improved by the wake galloping vibrations in comparison with a single PEH. The maximum open circuit RMS voltage produced was 27.65 V and the device maximum voltage output density was 77.45 V/cm^3.

Yan et al. [146] utilized crescent- and D-shaped bluff bodies inspired by the wake galloping of iced conductors. Wake galloping EHs with iced D-shape and crescent-shape bluff bodies (Figure 11d) exhibit a substantial boost in terms of captured power when compared with energy harvesters positioned in the wake of a non-iced circular bluff body. The output power could be enhanced 20 times more than a conventional galloping energy harvester, as suggested by Kim et al. [147]. The primary cause of such a performance boost was due to the synergistic impact of the interference wake. Yuan et al. [148] developed a TEEH driven by wake galloping that can harvest breeze wind energy. At a wind speed of 1.8 m/s, a cylindrical blunt body was utilized to achieve an output power density of 149 mW/m^2 at 100 MΩ. The TEEH converted and collected wind energy using a blunt body, and it had the advantages of a simple structure and high efficiency, making it ideal for usage at very low wind speeds.

Table 5 summarizes various energy harvesters based on the wake galloping mentioned above. Like the galloping phenomenon, most of the energy harvesters based on wake galloping in the literature were found to use the PE transduction mechanism. Optimization in terms of (i) bluff bodies (shape and dimensions) and (ii) distance between the upstream and downstream cylinders plays an important role in reducing the cut-in speeds, increasing the frequency bandwidth and maximizing the output generation.

Table 5. Summary of energy harvesters based on wake galloping.

Transduction Mechanisms	Cut-in Velocity (m/s)	Optimum Resistance (kΩ)	Velocity at Max Power (m/s)	Output Power (mW)	References
EM	1.2	0.007	4.5	370	Jung et al. [141]
PE	1.55	27,000	9.8	0.003195	Uttayopas et al. [143]
PE	1.5	500	2.36	0.8	Zhang et al. [144]
PE	-	4300	7.6	0.7	Yan et al. [146]
PE	2.45	410	9	2.3	Kim at al. [147]
TE	1	100	1.8	0.3	Yuan et el. [148]

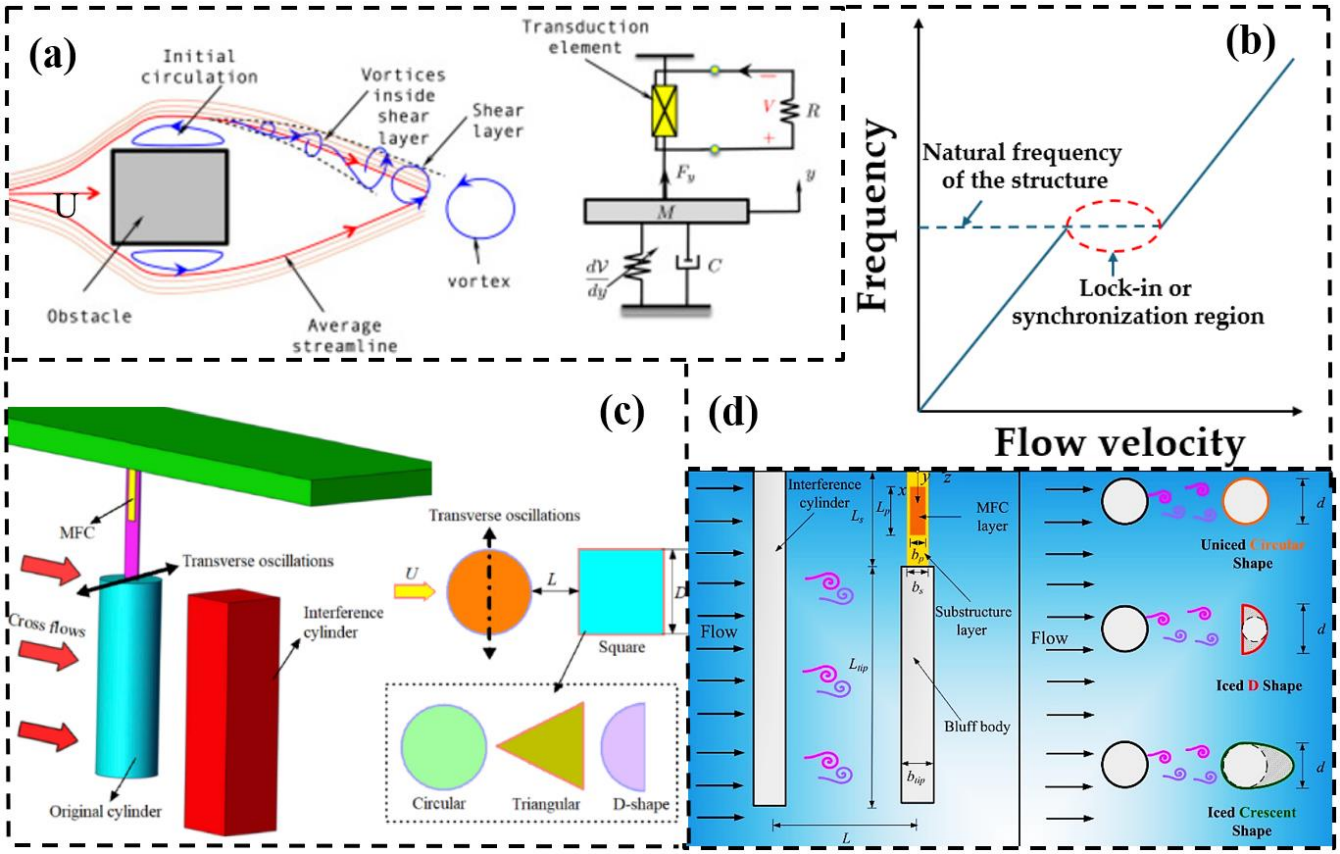

Figure 11. (**a**) Illustration of wake galloping phenomenon reproduced with permission from [136] Elsevier, 2016. (**b**) Characteristic response of wake galloping EH. (**c**) Wake galloping with different interference cylinder cross-sections reproduced with permission from [144] Elsevier, 2019. (**d**) Schematic of iced-conductor-inspired wake galloping reproduced with permission from [146] Elsevier, 2020.

7. Enhancement Methods to Optimize and Increase the Efficiency of FBEHs

The research articles discussed above highlight that aeroelastic energy harvesters have significant limitations: the decrease in efficiency due to the presence of variable wind speeds, which is unavoidable in the environment and limited performance within a narrow working wind speed range, along with an inability to generate adequate power for the continuous operation of autonomous electronic devices. Therefore, it is targeted to design and add features to FBEHs to broaden the working wind speed range, reduce the initial working wind speed and increase output power. To achieve these goals, researchers have proposed a variety of approaches to improve energy harvesting ability [149]. These involve integrating nonlinear forces, designing geometric nonlinear arrangements, creating multi-degree-of-freedom energy harvesters, developing multi-directional counterparts, and implementing interface circuits. Furthermore, the development of devices with hybrid transduction energy harvesting processes has been investigated. Researchers have investigated using coupled aerodynamic instabilities to increase overall efficiency. These ideas aim to overcome the challenges and issues encountered in the implementation of FBEHs.

7.1. Nonlinear FBEHs

Energy harvesters with linear structures face issues like susceptibility to damage and the need for high critical wind speeds to operate effectively. To overcome these, researchers have introduced nonlinear mechanisms, such as incorporating a nonlinear magnetic force, introducing nonlinear spring forces in the energy harvester design, establishing geometric nonlinear configurations, and exploiting bistable or multistable harvester designs. These nonlinear structures enhance energy conversion efficiency, broaden operational wind speed

ranges and improve durability. As a result, these achieve better performance under variable and lower wind speeds for environmental monitoring applications. This review focuses on nonlinear energy harvesters based on piezoelectric transduction techniques only, as these are widely explored in the literature for their compact design, scalability and higher energy density compared with other methods. Based on the FIV mechanism, several PE nonlinear energy harvesters are explained and compared in the following sections.

7.1.1. Nonlinear VIV-Based PE-FBEHs

Due to its distinctive characteristics of self-excited oscillations, maximum power is produced within the synchronization zone or (linear) resonance when vortex shedding frequency is near to one of the natural frequencies of the harvester's structure. VIV-based energy harvesting has gained significant attention; however, the narrow lock-in region of VIV energy harvesting is one of its major shortcomings. As the effectiveness of VIVs energy harvesters is optimum when vortex frequency approaches the natural frequency of the harvester, any variation in wind speed or vortex frequency causes a sharp reduction in the power. Contrarily, nonlinear harvesters use nonlinear characteristics to increase the frequency bandwidth, making them more robust and responsive to random and wide range vibrations [150]. Several such FEH configurations are depicted in Figure 12. Researchers are interested in the vibration response of VIVs energy harvesters reinforced by nonlinear springs. The primary characteristic of a nonlinear restoring force is that the concept of natural frequency does not exist. The system can excite a wider range of structural modes, introducing broadband frequency response. The limited frequency bandwidth of VIVs devices has been addressed from the perspectives of monostability, bistability and magnetic interaction. The nonlinear distributed parameter model was developed by Dai et al. [151]. They considered the first four modes of FEHs. A van der Pol wake oscillator was used as the basis for the concept of the lift force generated by VIVs. The study in [152] investigated improving wind energy conversion by utilizing a buckled beam vibration. Experiments have shown that when the buckling beam becomes unstable due to wind, it causes substantial vibration in the PVDF harvester, which results in significantly higher power output compared with traditional cantilever beam type harvesters.

To create an effective and broadband harvesting system, Naseer et al. [153] included attractive magnetic force (Figure 12a) to develop a nonlinear VIVs energy harvester, whereas Zhang et al. [154] incorporated nonlinear repulsive forces in their system. Two small magnets with repulsive forces were introduced, attached on the lower support and the bottom of a circular cylinder, respectively, and were subjected to a uniform wind speed. The dynamics of the energy harvester were affected by altering the relative positions of the magnets' center-line horizontal (Δx) and vertical (Δy) distances. Experiments revealed a significant increase in the dominating frequency of the energy harvester results in a wider synchronization region by 138% of the original configuration. The harvested power was gradually increased to the highest value of 150 μW (29% increase) at 3.2 m/s. Hou et al. [155] explored a cylindrical monostable EH based on vortex excitation. A maximum power of 0.21 mW was achieved at a flow velocity of 1.6 m/s. A self-aligning airfoil cantilever design adds nonlinear energy harvesting capabilities that can boost conversion efficiency. Although nonlinearities introduced in VIVs can greatly improve the output performance, there is a need for environmental adaptability and robustness from wind erosion. This issue was addressed by Wang et al. [156] by developing a non-contact PEH. Theoretical and experimental investigations were conducted on a piezoelectric transducer implanted in a cylindrical shell. The results showed that as the wind speed rose, the vibration amplitude and output were increased with an increasing transducer mass and decreasing shell mass. The research conducted in [157] introduced a nonlinearity in the system to design, develop and test a nonlinear airfoil-shaped PE-FBEH for VIVs as depicted in Figure 12b. The harvester converted FIVs from water into electrical energy. A passive self-adjustable base compensated for the changing flow direction that could reduce the conversion efficiency of energy harvesters. For misalignment correction, several beam

substrates were examined, with thin airfoil profiles able to orient more quickly at greater misalignment angles. An extra inline mode was detected for the same frequency range in low-velocity flow, outperforming the standard rectangular beams with similar volumes in the airfoil-shaped harvester. In the absence of flow misalignment, the piezoelectric MFC produced an average RMS output voltage of 132 mV for transverse oscillations.

Recently, Alimanesh et al. [158] investigated the nonlinear dynamic behavior of VIV-based PE-FEHs theoretically using a clamped–clamped beam; to create VIVs, two foam cylinders attached as a dumbbell were installed in the middle of the beam. The fluid interacted with the structure as it flowed over the cylinders, causing the system to oscillate and produce vortices behind the cylinders. The results show that middle layer stretching had a considerable impact on the lock-in domain and this effect was important while evaluating the output electric voltage. Likewise, Li et al. [159] investigated that the hardening stiffness effect can move frequency lock-in zones to higher wind speeds, hence increasing aerodynamic pressures and achieving wide wind speed bandwidths and large voltage outputs. The VIV energy harvester with nonlinear stiffness (Figure 12c) demonstrated a maximum voltage of 9.87 V with a frequency lock-in range of 2.27 to 5.36 m/s.

7.1.2. Nonlinear Galloping PE-FBEHs

In the case of galloping energy harvesters, many researchers have focused on the nonlinear techniques for a wider range of wind speeds and to reduce the critical speed for galloping to occur. Zhao et al. [160] studied a two-degree-of-freedom galloping energy harvester in which two magnets generated a nonlinear spring stiffness effect. In comparison to a conventional energy harvester, the harvester successfully extracted energy from the reduced wind speed and produced enhanced power. Bibo et al. [161] used a nonlinear restoring force. In their research work, the magnetic force was modeled as a nonlinear spring with a quadratic potential energy function that, due to its bistable property, can exhibit spring softening and hardening effects. Similarly, another bistable EH was developed by Zhao et al. [162] by utilizing Y-shaped curved wings as illustrated in Figure 12d. The results conclude that coherent large vibration amplitudes can be attained across various airflow velocity ranges. Tan et al. [163] suggested an effective configuration for the resistor, inductor and supercapacitor to identify the optimized RLC circuit that concurrently attributes the best electrical damping and tolerable inductance for improved electrical impedance in galloping energy harvesting systems. Through theoretical predictions and wind tunnel tests, by adding the supercapacitor to the galloping system at low-velocity wind, the harvester's power generation increased by 450%. However, there is a need to reduce the cut-in wind speed for low-frequency applications. Kai Yang et al. [164] developed a double-beam piezo-magneto-elastic energy harvester for which the critical wind speed to activate the galloping vibration was decreased by 41.9%. The prototype consisted of two piezoelectric beams, both supported by a prismatic bluff body. To create a bistable nonlinearity, the tip magnets were positioned so that the magnets repelled one another. This significantly dropped the critical wind speed. A PE-FBEH based on tristable galloping was fabricated [165] by adding a nonlinear magnetic force to the conventional galloping-based energy harvester. According to numerical findings, at a wind speed of 7 m/s, a maximum output power of 0.73 mW was reported.

Many researchers have developed theoretical models for galloping-based energy harvesters and validated them for optimization in realistic environments. A multi-field nonlinear model for environment-coupled galloping energy harvesting was established in [89]. The wind tunnel was divided into sections for power generation, flow stabilization, flow contraction, harvester testing and flow diffusion. Through the contraction region, the incoming airflow's velocity was increased to the trial speed of up to 30 m/s. The flow state gradually changed from laminar flow to turbulence as the wind speed increased. Three cross-sectional shapes of the bluff bodies, a semicircle, a triangle and a trapezoid were tested; all had the same height, width and mass and were positioned windward. The trapezoidal bluff body produced superior aerodynamic and energy harvesting capabilities. With

the environment's adaptable load resistance, the cut-in galloping speed of the harvester was reduced to lower than 1 m/s for the galloping to occur. A PE-FBEH with a sliding bluff body introducing nonlinear spring configuration was proposed by Sun et al. [166]. Figure 12e illustrates that the bluff body was made to move in the axial direction while being restrained by an elastic beam, and a set of springs was attached in between. The imbalance between the drag, centrifugal force, spring and friction forces governed the motion of the bluff body. The effect of the sliding bluff body (distance traveled = effective beam length) on the performance of the harvester was investigated in terms of critical wind velocity, transverse displacement, average power and power density. The findings demonstrate that, as compared to the traditional harvester with fixed bluff body, this PE-FBEH exhibits exceptional energy harvesting performance. A similar nonlinear approach of asymmetric magnetic coupling was introduced by Zhang et al. [167]. The piezoelectric beam experienced simultaneous bending and torsional vibration due to the eccentric distance. Experiments at various eccentric distances and wind speeds demonstrated the optimal external load resistance. The asymmetric magnetically coupled galloping energy harvester had a lower threshold wind speed of 2 m/s. The maximum output power at 6.4 m/s was about 5.5 mW at an optimum resistance of 100 kΩ for the reported harvester.

To improve the functional performance of aeroelastic energy harvesters in environments with varying wind speeds, a dual-beam piezoelectric wake-induced EH was reported in [168]. The device consisted of two piezoelectric beams connected by magnets (creating upstream and downstream EHs), with each beam attached to a cylindrical bluff body. When wind speed exceeded a crucial value, the displacement and voltage amplitudes increased significantly. The wind speed threshold value was about 1.25 m/s. When the wind speed and magnet separation were 10.2 m/s and 20 mm, respectively, the system's output power reached 0.49 mW.

7.1.3. Nonlinear Flutter PE-FBEHs

The performance of flutter-based energy harvesters can be enhanced in a variety of ways, for example, by the addition of nonlinearities. The harvester's bandwidth can be widened, allowing it to produce energy for a broad range of wind speeds due to the presence of multi-resonances. Since nonlinearities can produce a subcritical Hopf bifurcation, the cut-in wind speed of the harvester can be reduced. Moreover, the harvester's capacity to capture energy can be amplified. This is mainly due to the chaotic vibrations caused by additional nonlinearities in flutter energy harvesters, which can improve the energy transmission between the structure and the piezoelectric component. The impacts of the structural nonlinearities of the PE-FBEH were examined theoretically and experimentally by Sousa et al. [169]. It was demonstrated that the cubic hardening stiffness contributed to sustained oscillations with appropriate amplitude over a broad spectrum of flow velocities.

The combined nonlinearities were investigated analytically by taking advantage of freeplay nonlinearity [170,171]. Orrego et al. [172] examined the application of a passive self-aligning mechanism to account for shifting wind directions in an inverted flag introducing nonlinear behavior. At a wind speed of 9 m/s, 5.0 mW/cm^3 power density was obtained. Even in low-wind speed regimes (3.5 m/s), the harvester was ideal for ambient wind energy collection and was capable of producing a power density of 0.4 mW/cm^3. In addition, a self-aligning system was incorporated to account for fluctuating wind directions that did not cause any hindrance in powering the sensors. With the harvester's enhanced power, the data output of the operated sensor was increased by 20 times. These results provide new possibilities for autonomous devices under variable conditions and low wind-speed environments. Wu et al. [173] numerically investigated a double-plunge-degree-of-freedom PE-FBEH via the dynamic stall model. Their findings reveal that the cut-in wind speed was lower and the output power was larger than those of the single-plunge-degree-of-freedom PE-FBEH. A dynamic multistable harvester for flutter energy was proposed by Zhou et al. [174] and achieved snap-through and high-power output (at 1.5–7.5 m/s wind speeds).

Magnetic nonlinearity was incorporated into the PE-FBEH design by Li et al. [175,176]. A flutter EH with a flap was proposed by Elahi et al. [177]. The flap was easier to incorporate nonlinearity than the airfoil structures. The developed EH had a maximum power generation of 5.5 mW. Tian et al. [178] carried out a comparative analysis of unsteady aerodynamic loads and dynamic stall models. The results predicted the unsteady aerodynamic model was more accurate in terms of output performance. To simulate the plunging motion of a typical airfoil, Tian et al. [179] utilized two flexural springs symmetrically attached to the airfoil shaft and the holder. The two flexural springs allowed for periodic bending and deformation perpendicular to the airflow. By incorporating the cubic structural stiffness coefficient, the maximum output voltage was 29.08 V and the maximum output power was 3.382 mW, which demonstrates the improved energy harvesting performance. Recently, Velusamy et al. [180] investigated the feasibility of using a bistable dual cantilever for flutter energy collecting. Two identical pole magnets were linked to the free ends of the cantilever to create a bistable effect on beams. The bistable state of the beams showed 2.5 times increase in amplitude of oscillations compared with monostable beams. The energy harvester design shown in Figure 12f is a tristable flutter energy harvester reported by Li et al. [181]. It is capable of large amplitude interwell plunging displacements and high-performance energy harvesting. Five vibration forms were observed, including intrawell limit cycle oscillations (LCOs) in the first, second and third wells, and additionally aperiodic responses, and interwell LCOs between the three potential wells. The experiment yielded a peak-to-peak voltage of 28.17 V at 15.5 m/s.

Table 6 lists and compares nonlinear energy harvesters based on aerodynamic instabilities, i.e., VIV, galloping and flutter. Nonlinearities are categorized as magnetic nonlinearities, resulting in monostable, bistable and tristable energy harvesters. Nonlinearities are mainly induced to increase the frequency range. Understanding and leveraging magnetic-induced nonlinearities is critical for improving energy harvesting efficiency. Spring structures and cubic spring stiffness are included in the design of energy harvesters, giving rise to nonlinearities. Such designs including nonlinear elements allow for greater flexibility and responsiveness to changing environmental circumstances, hence improving the device's overall performance in these conditions.

Table 6. Summary of nonlinear PE-FBEHs.

Type of FIV	Nonlinearity	Optimum Resistance (kΩ)	Velocity at Max Power (m/s)	Output Power (mW)	References
VIV	Buckled beam	1000	14	0.0618	Zhang et al. [152]
	Magnetic nonlinearity	50	3.2	0.15	Zhang et al. [154]
	Magnetic coupling monostable	500	1.6	0.21	Hou et al. [155]
	Non-contact PEH	300	40	1.438	Wang et.al [156]
Galloping	Magnetic nonlinearity	600	7	0.73	Wang et al. [165]
	Nonlinear spring configuration	504	4	35	Sun et al. [166]
	Magnetic nonlinearity	100	6.4	5.5	Zhang et al. [167]
	Magnetic nonlinearity	1000	10.2	0.49	Ma et al. [168]
Flutter	Cubic stiffness nonlinearities	100	18	106	Sousa et al. [169]
	Self-sustained inverted flag	10,000	9	5 mW/cm^3	Orrego et al. [172]
	Magnetic force-induced nonlinearity	1000	3.1	0.07	Li et al. [175]
	Structural nonlinearity	100		5.5	Elahi et al. [177]
	Structural nonlinearity	250	15.16	1.27	Tian et al. [178]
	Structural nonlinearity	250	14	3.382	Tian et al. [179]

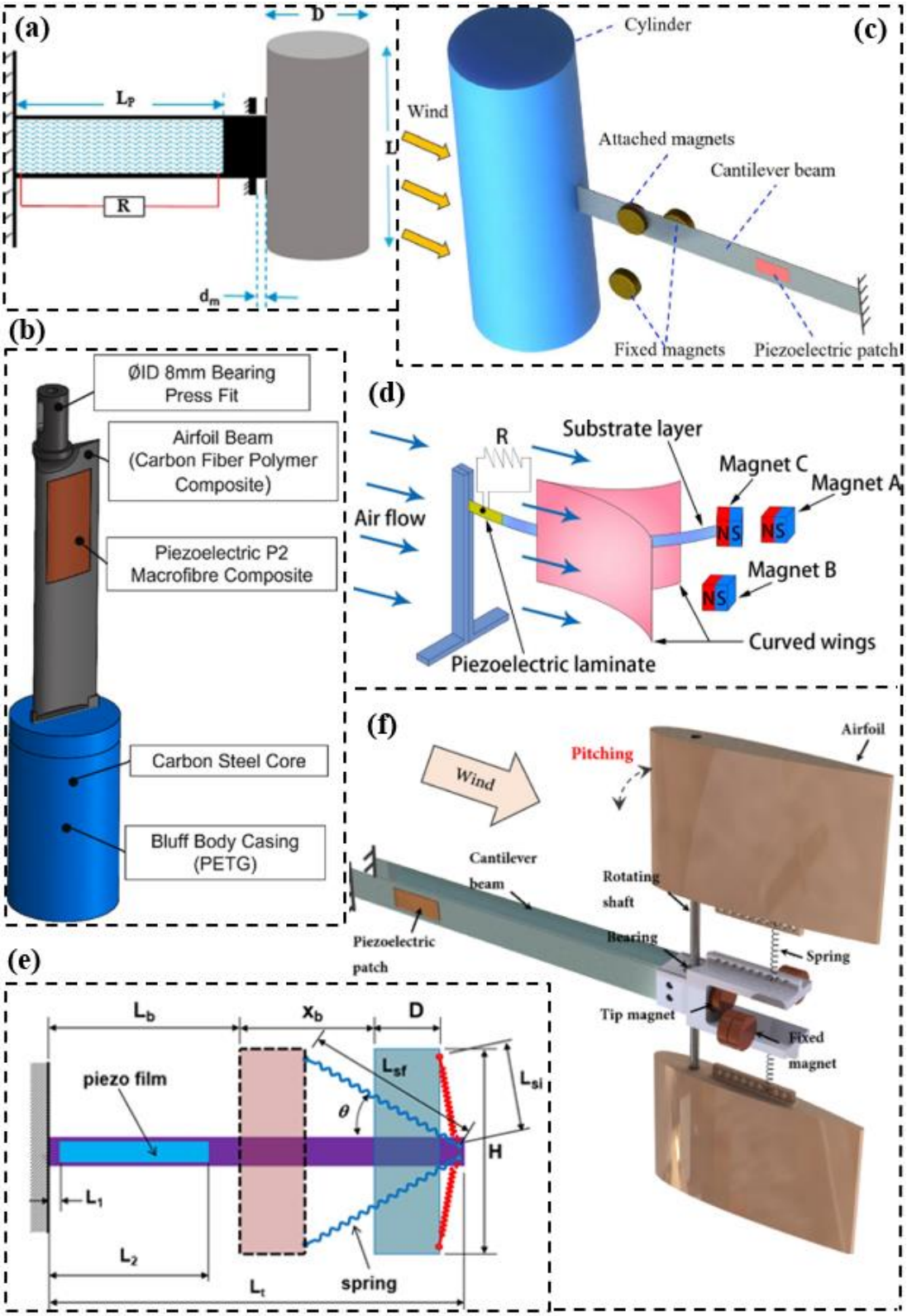

Figure 12. Nonlinear PE-FEHs: (**a**) VIV piezo-magneto-elastic EH reproduced with permission from [153] Elsevier, 2017. (**b**) Self tunable airfoil EH [157]. (**c**) VIV-EH with nonlinear stiffness reproduced with permission from [159] Elsevier, 2024. (**d**) Y-shaped bistable PEH reproduced with permission from [162] Elsevier, 2018. (**e**) Galloping-based moving bluff body reproduced with permission from [166] Elsevier, 2021. (**f**) Tristable flutter-based PEH reproduced with permission from [181] Elsevier, 2024.

7.2. Multi-Transduction Mechanisms: Hybrid Flow Energy Harvesters (HFEHs)

Researchers focusing on expanding the frequency range of FEHs are also working to increase the voltage and power levels of the harvester. Hybrid flow energy harvesting [182] is one of the techniques which combines numerous transduction mechanisms, i.e., EM, PE and TE or simultaneously extracts two or more ambient energies. Multi-transduction techniques integrated into a single unit can create more power across a wider band of frequencies, increasing its adaptability and efficiency in obtaining energy from various sources. This method offers novel opportunities for more adaptable and effective FEHs. Combining PE and EM harvesting mechanisms concurrently benefits from the advantages of both. According to tests conducted by Vinod et al. [183] on the hybrid piezoelectric–electromagnetic energy harvesters, the output power of a hybrid energy harvester is greater than that of a single piezoelectric or electromagnetic energy harvester. Zhao et al. [184] developed a new piezoelectric–electromagnetic hybrid flow energy harvester (HFEH) based on VIVs in water flow. The experimental findings demonstrate that the HFEH outperforms the single transduction energy harvesters in terms of power generation. Under the combined impacts of the dual transduction, the maximum power of 16.55 mW was attained when the attached resistances were 400 kΩ and 2.2 kΩ for the piezoelectric and electromagnetic parts, respectively. A high-efficiency energy harvesting windmill with the capacity for power delivery and quick charging was proposed by Rahman et al. [185]. The reported harvester was based on three conversion mechanisms: piezoelectric, electromagnetic and triboelectric conversion. Javed and Abdelkefi [186] investigated that the positioning of a magnet on a piezo-cantilever beam has a large impact on the synchronization region and power generation. Wang et al. [187] proposed a galloping energy harvester utilizing piezoelectric and triboelectric transduction. The PEH would begin operations in the low wind zone. As the wind speed increased, the TEEH would begin to work along the PEH. The TEEH safeguards the piezoelectric material from damage in high wind speeds and improves the performance in terms of increased output broadening the working speed range. Total power generated by the device was 2.3 times that of the PEH alone; for the harvester a power of 0.24 mW at 14 m/s was reported.

A magnetic coupling force was used by Li et al. [188] to combine a flutter-based PE-FBEH and a linear spring-type electromagnetic energy harvester, which significantly decreased the cut-in wind speed and improved harvesting performance. Mahmood et al. [189] proposed a PE-EM hybrid energy harvester. They used a cylindrical blunt body fixed to the end of a piezoelectric cantilever beam and embedded the magnetic coil inside the cylindrical blunt body, suggesting a more efficient and compact system. Li et al. [190] reported a flutter HEH with outstanding performance. The nonlinear behavior of the harvester was analyzed. Compared with a conventional flutter-based FEH, the device produced more power and had a lower cut-in wind speed. At a wind speed of 6.70 m/s, the piezoelectric and electromagnetic components had output powers of 1.35 mW and 36.63 mW, respectively. Along with other nonlinearities, the HEH can be utilized in multistable configurations; for example, Li et al. [191] proposed a magnetically coupled hybrid galloping energy harvester. The bistable nonlinear device comprised PE and EM components. The higher the degree of coupling, the more dominant were the nonlinear features. The results demonstrate that the onset wind speed and output power are superior to those of the conventional galloping PE-FBEHs. When the wind speed was 11 m/s, the onset wind velocity was decreased by 28% and the output power was enhanced by 136%.

Table 7 summarizes some of the HFEHs. The multiple energy harvesting mechanisms offer several benefits compared with single mechanism EHs. They contribute to increased efficiency and energy output, as seen in [184]. Moreover, at a very low velocity, the output achieved was greater when compared to standalone PEHs since these struggle to capture energy at low velocities. With the addition of electromagnetic components along the PE transduction, the efficiency of the HFEH is comparatively high. Likewise, in [185], the electromagnetic part had the highest contribution to output obtained. Additionally, in HFEHs, when the system gains impulse from the wind flow, the PE, EM and TE harvesters generate

electricity simultaneously. The combined electrical output produces a greater total power output in HFEHs. This improved power generating capability is especially useful for long-term and energy-intensive applications, allowing for dependable operation over extended periods. HEHs operating concurrently provide more redundancy. Furthermore, if one harvester encounters problems or loses efficiency, the others can compensate, resulting in a more reliable and robust energy harvesting system for continuous monitoring applications.

Table 7. Hybrid flow energy harvesters.

Harvester Type	Optimum Resistance (kΩ)	Velocity at Max Power (m/s)	Output Power (mW)	References
VIVs	400 (PE) 2.2 (EM)	0.6	16.55	Zhao et al. [184]
Rotational	10,000 (TEEH) 330 (PE) 180 (EM)	6	1.67 (TEEH) 1.38 (PE) 286.6 (EM)	Rahman et al. [185]
VIVs	1 (PE) 0.01 (EM)	1.8	0.7375 (PE) 0.095 (EM)	Javed et al. [186]
Galloping	2000 (PE) 100,000 (TEEH)	14	0.1 (PE) 0.07 (TEEH A) 0.064 (TEEH B)	Wang et al. [187]
Flutter and vibration	160 (PE) 0.04 (EM)	14.5	4.4 (PE) 3.68 (EM)	Li et al. [188]
Flutter	150 (PE) 0.419 (EM)	6.7	1.35 (PE) 36.63 (EM)	Li et al. [190]
Magnetically coupled Galloping	750 (PE) 0.05 (EM)	11 7.15	1.79 (PE) 3.92 (EM)	Li et al. [191]

7.3. Coupled Fluid Flow Phenomena

It is a challenging but promising field to integrate aeroelastic instabilities to utilize the combined effects of several aerodynamic instabilities for flow energy harvesting. More effective and sustainable energy generation systems can be designed and comprehended by combining different fluid flow phenomena. Aeroelastic instabilities can be combined in a variety of ways; that is, by utilizing various FIV mechanisms inside a single energy harvester or at different stages of the energy harvesting process, the performance can be enhanced. For example, during the energy harvesting process, the first vibrations could, for instance, be produced by flutter, and then could be amplified by VIVs. Similarly, researchers have pointed out that VIVs, galloping and wake galloping can be intercoupled to improve the performance of FEHs.

7.3.1. Interaction of VIVs and Galloping

In the case of coupled vortex excitation and galloping, the natural frequency of the system is close to the vortex shedding frequency. This frequency can amplify the oscillations of the structure and lead to galloping. Usually, the VIV happens first, and as the wind speed rises, galloping occurs. Additionally, combining both phenomena causes vigorous vibrations. Combining VIVs with galloping to improve wind energy harvesting performance has recently gained attention and popularity. A thorough phenomenological explanation of the VIV-galloping interaction mechanism was provided by Mannini et al. [192]. The study showed the coupled and decoupled situations of the VIV–galloping interaction. The fabricated prototypes fall into two primary categories. One contends that the aerodynamic properties of a circular cylinder can be changed by adding structural attachments, leading to galloping or a hybrid of VIVs and galloping rather than a pure VIV-based harvester. Hu et al. [193] developed a wind-based PEH which could benefit from the interaction between

VIVs and galloping. A circular-based PEH with three various small-size attachments (circular, triangular and square), as shown in Figure 13a, was tested. They concluded that, when compared with the other two varieties, the triangle rod attachment at an angle of 60° outperformed. He et al. [194] presented an experimental technique to show the separation or superposition of a VIV and galloping by changing the aspect ratio of a rectangular cylinder. In order to improve performance over a wider range of wind velocities, a T-section fin FEH was subjected to the vortex shedding–galloping coupled mechanism [195]. Sun et al. [77] discussed how to combine VIVs and galloping to increase the effectiveness of extracting wind energy through the synergetic interaction of two typical geometries: circular and rectangular cylinders. Figure 13b explains the dynamic interaction between VIVs and galloping for energy harvesting. As wind speed increases from point 1 to point 2, VIV lock-in dominates, followed by a decrease in oscillation amplitude, reaching equilibrium at point 6. At point 5, galloping causes a sudden amplitude jump to point 4, and then gradually decreases to point 3 before dropping to equilibrium. Upon further speed reduction, the VIV reappears before the system returns to rest, showing a subcritical bifurcation and hysteresis effects. A conventional galloping-based FEH typically employs a prismatic bluff body while a standard VIV energy harvester often utilizes a cylindrical bluff body. To combine both effects, Qin et al. [196] utilized a cross-shaped beam along a cylindrical bluff body and two cuboid bluff bodies shown in Figure 13c. Similarly, in [197], a novel bluff body with rounded and folded corners superimposed galloping and VIV effects. According to the experimental findings, the harvester's voltage output reached 14.6 V when it had a half cuboid and half cylindrical bluff body. The introduction of a dumbbell-shaped bluff body presented in [198] integrated higher amplitudes during galloping and a lower cut-in speed for the VIV depicted in Figure 13d. Ding et al. [199] evaluated the performance of the wind-induced vibration cylinder with fin-shaped rods (FSRs) for energy harvesting. Their findings demonstrate that the output power of cylinder-based aeroelastic energy harvesters can be greatly increased by the proper installation of FSRs on a bluff body.

However, all these investigations consider changing the bluff body geometry. Ding et al. [45] developed physical models for circular cylinders with passive turbulence control (PTC), square, trapezoid and triangular prisms and observed VIVs combining with galloping. Kan et al. [46] inserted a downstream diamond-shaped baffle to change the aeroelastic instability of the cylindrical bluff body. By including the piezoelectric transducer inside the cylindrical shell (bluff body), the system also gained an advantage from the indirect interaction between the PEH and the wind. Recently, Xing et al. [200] reported another way of coupling the VIV and galloping effect, i.e., by introducing protrusions on the surface of the bluff body and finding an optimum aspect ratio for the bluff body. The cut-in velocity varied for each scenario. Experiments revealed that at a wind speed of 5.1 m/s, the maximum output power from the analyzed scenarios was 0.992 mW for a 3:2 aspect ratio of the bluff body and protrusion length of 10 mm.

All the above studies incorporate only one cylinder to generate wind energy; however, Kim et al. [147] utilized the synergistic effect of the transverse and interference galloping phenomenon. They installed an interference in the shape of mirror symmetry with respect to the bluff body. The developed harvester's output performance was compared to that of a traditional transverse galloping-based PEH. The coupled synergistic impact resulted in an electrical power almost 20 times greater than that of the traditional galloping FEH.

Chen et al. [201] proposed a 2-DOF coupled VIV and wake galloping FEH by utilizing two parallel and elastically connected cylinders. The cylinder facing the wind flow, i.e., the windward cylinder (bluff body 2) or the leeward cylinder (bluff body 1), matched the first or second natural frequency resonance during operation, and the system underwent VIVs. However, at relatively high wind speeds, VIVs convert to wake galloping and scavenge wind energy in a wide range of wind velocities with two lock-in regions.

7.3.2. Coupled Flutter and VIVs

Researchers are investigating the complex phenomenon known as coupled flutter-VIV. Systems with combined flutter and VIVs can serve as a promising solution for self-powered applications. The literature so far mentioned cantilever beam-mounted flutter-induced PEHs. Shan et al. [202] proposed a composite energy harvesting method to simultaneously capture flutter and VIVs. The flutter-induced harvester connected the cantilever beam to the oscillating airfoil and the effect of several springs on the output response was demonstrated. Additionally, a cylindrical bluff body was attached to the free end of the cantilever. The airfoil underwent flutter vibration, and the bluff body (cylinder) captured the vortex excitation. This coupling effect boosted the energy harvesting performance. At a wind speed of 14.48 m/s, an output power of 154 μW was reported. A cylinder with two symmetrical airfoils on both sides was designed as a nonlinear vortex-induced flutter PEH [203], as shown in Figure 13e. The assembly of two airfoils connected with a shaft to the cylindrical bluff body was then attached to a cantilever beam, enabling the flutter–VIV coupling. This approach significantly enhanced the output of the harvester, which was 6.47 mW, whereas the maximum output of the harvester, individually based on VIVs and flutter, was only 0.05 mW and 0.26 mW, respectively.

To improve the vibration and energy harvesting performance, Wan et al. [204] developed a novel kind of aeroelastic PEH. The flap was fastened to the trailing edge of the airfoil and tested two ways. Firstly, the flap was constrained by a spring rod and rotated at small angles; secondly, the flap was unconstrained by removing the spring rod and rotating freely. The change in vibration mode from flutter to VIV is an important finding from theoretical, computational and experimental examinations. The output power of 5.43 mW can be harvested at 14.39 m/s during unconstrained conditions.

Table 8 summarizes different types of coupled energy harvesters based on different FIV phenomena. Based on the FEHs discussed in this section, the VIV–galloping coupling effect was achieved by varying dimensions or amending the features of a bluff body in terms of aspect ratios [200]. The VIV has a limitation in terms of bandwidth, which refers to the range of frequencies over which the energy harvester can operate. The transition from VIVs to galloping offers a solution to overcome this limitation by expanding the frequency range in which the harvester can effectively operate. This increased flexibility enables better adaptability to varying fluid flow conditions, making the energy harvesting system more reliable and applicable to a wider range of applications. In some cases, an additional bluff body is introduced [201], to achieve a coupled VIV–wake galloping with two cylinders elastically connected. As a result, at low wind speeds, it can exhibit resonant oscillations when the vortex shedding frequency matches the first or second natural frequency, whereas, at relatively high wind speeds, it can engage in wake galloping and scavenge wind energy over a wide wind speed range, with both cylinders contributing to higher power output. This resonance can enhance the energy extraction efficiency, as it allows the system to synchronize with the incoming wind, effectively capturing more energy from the fluid flow. Similarly, the flutter–VIV coupled energy harvesters in [203,204] also influenced the output of the harvesters. By coupling these two instabilities, the system could take advantage of the strengths of each instability mechanism, optimizing energy extraction consistently across varying wind conditions and making the overall energy harvesting process more effective.

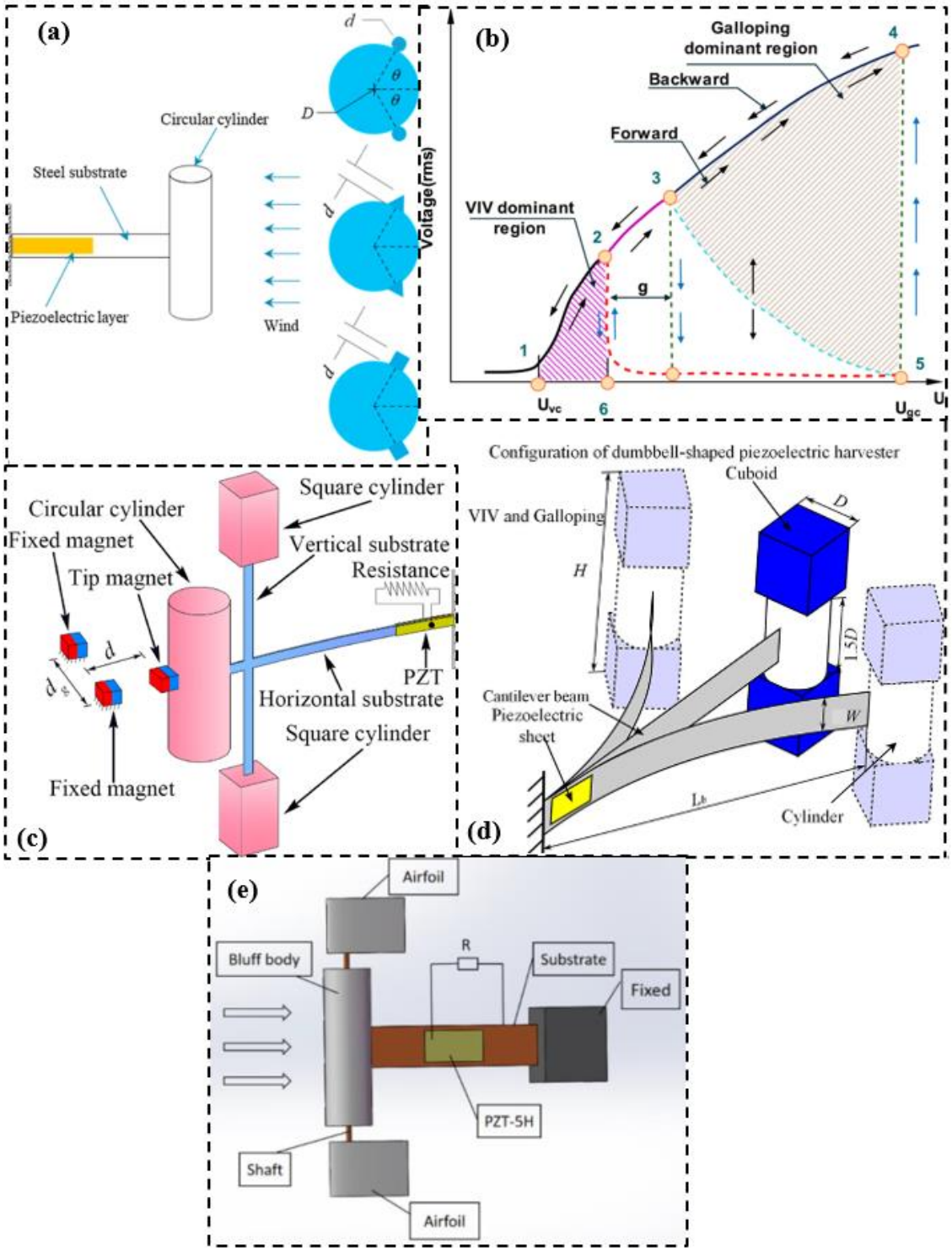

Figure 13. Coupled fluid flow phenomena in FEHs: (**a**) circular-based PEH with attachments (circular, triangular, and square) reproduced with permission from [193] Elsevier, 2018; (**b**) interaction between VIV and galloping in FEH reproduced with permission from [77] Elsevier, 2019; (**c**) VIV and galloping PEH reproduced with permission from [196] Elsevier, 2019; (**d**) dumbbell-shaped bluff body for FEH reproduced with permission from [198] Elsevier, 2024; (**e**) cylindrical bluff body in FEH with two symmetrical airfoils [203].

Table 8. Energy harvested based on multiple FIV phenomena.

Coupled Mechanism	Shape of the Bluff Body	Cut-in Velocity (m/s)	Optimum Resistance (kΩ)	Velocity at Max Power (m/s)	Output Power (mW)	References
VIV–Galloping	Diamond-shaped baffle		200	32	-	Kan et al. [46]
VIV–Galloping	Bulb-shaped		50	2.95	-	Sun et al. [77]
Galloping–Wake galloping	D-shaped	2.45	410	9	2.3	Kim et al. [147]
VIV–Galloping	T-shaped	<2	1500	3	0.4	Petrini et al. [195]
VIV–Galloping	Fin-shaped		200	6.8	1.645	Ding et al. [199]
VIV–Wake galloping	Cylindrical-shaped	(i) 0.8 (ii) 2.5	(i) 1000 (ii) 250	6.5	0.00875	Chen et al. [201]
VIV–Galloping	Rectangular with leeward protrusion	2	200	5.1	0.992	Xing et al. [200]
Flutter–VIV	(i) Airfoil (ii) Cylinder	5.42	400	14.48	0.154	Shan et al. [202]
Flutter–VIV	Cylindrical with two airfoils	4.8	140	9	6.47	Li et al. [203]
Flutter–VIV	Airfoil	7.6	250	14.39	5.43	Wan et al. [204]

8. Rotary Wind Energy Harvesters

A rotary wind energy harvester (RWEH) is a device that converts wind energy into mechanical energy (rotating motion) and then into electrical energy. This technology is commonly used to extract wind energy with rotating rotors, like wheels, turntables and turbines. Scholars have performed extensive research on RWEHs due to their significant potential for environmental monitoring. Due to randomness of environmental wind energy sources, the use of RWEHs for self-powered sensing has become a viable and realistic solution in the context of environmental condition sensing and monitoring [205]. The challenge in designing such RWEHs is to enhance energy gathering efficiency over a large wind-speed range and in multiple directions.

Figure 14a illustrates a rotational PEH presented by Zhang et al. [206]. The blowing wind causes the fan blade and turntable to rotate. The turntable impacts the PVDF beam, causing it to vibrate. The harvester can efficiently scavenge wind energy. At a 14 m/s wind speed, the RMS voltage of 160.2 V with a maximum output power of 2566.4 μW was achieved. Fan et al. [207] suggested a hybrid RWEH that can be used to capture wind energy. The device mechanism comprises a spinning body and a sliding body, as shown in Figure 14b. The complete power production system is composed of TEEHs on the sliding body and an EMEH in the rotating body. The voltages of the TEEH and the EMEH are 416 V and 63.2 V, respectively, at the wind speed of 15 m/s. The output performance of TEEHs and EMEHs rises with increasing wind speed. The highest output powers of the TEEH and EMEH are 0.36 mW and 18.6 mW, respectively, at a wind speed of 9 m/s. Li et al. [208] reported a hybrid RWEH that combined a rotating EM component with a soft friction and positive-directional TEEH. The distinctive design overcomes the oscillating output of traditional TEEHs and enables consistent, positive energy output. The layered design of the harvester maximizes the use of wind energy for greater output. This configuration enables IoT sensor nodes to monitor the forest environment, enabling the wireless collection and transmission of temperature and humidity data, ultimately assisting in the prevention of forest fires.

Figure 14c [209] depicts a hybrid RWEH, which employs PE, EM and TE mechanisms. The design approach focused on low-frequency wind speed to increase electrical output. The plucking units were designed to reduce the number of strips plucked per time, resulting in a lower start-up wind speed. The rotational EMEH was crucial to the design. The piezoelectric materials were distributed in a circular pattern along the inner area of the outer shell. The TEEH was incorporated at the interface between the outer layer of the inner case and the inner layer of the device. At a 3.5 m/s wind speed, the PE, EM and TE components produced maximum electrical powers of 121 μW, 191 μW and 168 nW, respectively.

The study in [210] designed a low wind-speed piezoelectric windmill type RWEH with five blades, and a magnetic force was utilized to stimulate the piezoelectric cantilever beam. A shaft carrying the hub (holding the magnets) translated the shaft's angular motion into a vibration of the piezoelectric cantilever. The harvester produced powers of 1.06 and 2.21 mW at wind speeds of 2 and 5 m/s, respectively.

Cao et al. [211] developed a high-performance hybrid RWEH by coupling EM and TE mechanisms for ocean wind energy harvesting. By introducing an energy management circuit along the electromagnetic component, the charging efficiency of the TEEH was enhanced by 15 times. The all-in-one device structure can be installed on a lighthouse or the deck of a cruise ship to easily gather oncoming ocean wind energy. The energy harvester was made up of two freestanding mode TEEHs, top and lateral, and a rotary-structured bottom EMEH to fully utilize and harvest ocean wind energy.

Most contemporary wind-induced vibration energy harvesters are unidirectional and insensitive to changing wind direction. To address the challenge, Li et al. [212] offered an orientation-adaptive EMEH. The EH consists of a rotating bluff body, an elastic beam, a cylinder, a round-shaped magnet and coils array, as shown in Figure 14d. When the wind blows in any direction, the design structure can turn adaptively, exciting the cylinder sleeve and causing VIVs. It vibrates perpendicular to the wind, causing the permanent magnet to oscillate back and forth above the wound coil array, allowing the coils to cut magnetic induction lines and produce electric current. It was observed when the beam stiffness was large, increasing the rotatory inertia of the rotatable bluff body maximized the EMEH's output performance. Experiments revealed that an output power of 0.673 mW was obtained at a wind speed of 8 m/s.

Li et al. [213] reported a TE-based RWEH with soft-contact operating mode, which was developed with tunable contact areas by utilizing the consistent thermal response of Nickel titanium (NiTi) shape memory alloy (SMA) to air/wind temperature. The device demonstrated promising application as a power source with an average power density of 140 mW/m^2 at the wind speed of 12 m/s. This was demonstrated as a power source for online monitoring sensors, self-powered wind speed sensing and airflow temperature monitoring.

Table 9 represents various wind driven RWEHs operating on PE, EM, TE or multiple transduction techniques. These energy harvesters can be widely utilized in renewable energy systems, including wind turbines and hydroelectric generators. These EHs have a simple and compact design which can help to reduce maintenance requirements. In [207], EM- and TE-based RWEHs can be enclosed in a compact structure. Additionally, optimizing the TE materials ensures increasingly consistent and sustainable sources of energy over time. It is worth mentioning that EM RWEHs usually produce larger output power than clearly realized in Table 9. The fundamental advantage of RWEHs is their ability to operate effectively in multiple directions, which allows them to efficiently gather energy from a variety of sources, including vibrations and rotations, independent of the direction of input wind motion. The wind direction varies regularly in natural settings; most traditional PEHs can only gather wind-induced vibration energy from one direction and cannot use it in multiple directions. This flaw was addressed by the research in [212]. The RWEH is usually capable of collecting wind energy from all directions, with considerable output power, which is critical for resolving the issue of harvester's performance in multi-wind directions.

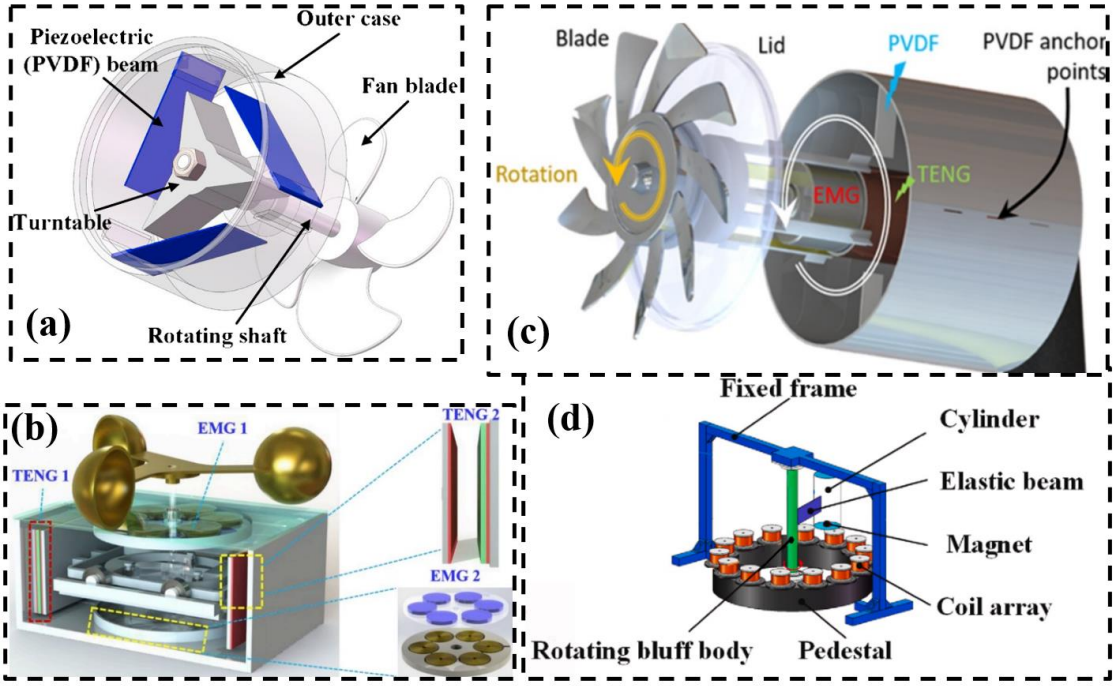

Figure 14. Rotary wind EHs: (**a**) TE-PE energy harvester reproduced with permission from [206] Elsevier, 2017; (**b**) TE-EM energy harvester reproduced with permission from [207] Elsevier, 2020; (**c**) PE-EM-TE-based RWEH reproduced with permission from [209] Elsevier 2022; (**d**) orientation adaptive EM-based RWEH reproduced with permission from [212] Elsevier 2024.

Table 9. Comparison of rotary wind energy harvesters.

Transduction Mechanism	Velocity (m/s)	Output Power (mW)	References
Tribo-electromagnetic	9	0.36 (TE) 18.6 (EM)	Fan et al. [207]
Piezoelectric-triboelectric-electromagnetic	3.5	0.121 (PE) 0.191 (EM) 0.000168 (TE)	Egbe et al. [209]
Piezoelectric	2	1.06	Narolia et al. [210]
	5	2.21	
Tribo-electromagnetic	15	7.54 (Lateral TE) 7.85 (Top TE) 22.5 (EM)	Cao et al. [211]
Electromagnetic	5.22	0.498	Li et al. [212]
	8	0.673	
Triboelectric	12	140 mW/m^2	Li et al. [213]

9. Discussion, Future Prospects and Challenges for FBEHs

This research discusses FIVs and aerodynamic instabilities employed for energy harvesting technology. In retrospect, the literature shows that several types of harvesting procedures have made tremendous progress in the last few decades. The applications of these FIV systems have been used to lessen reliance on traditional energy sources, such as chemical batteries, etc. Furthermore, the viability of the energy harvesting principle enables a safer environment and consistent energy for remote sensing and monitoring systems. Harvesting vibration energy from induced aerodynamic instability phenomena,

such as VIVs, galloping, flutter and wake galloping are typical crossflow vibration-induced aerodynamic phenomena that are considered for energy harvesting applications at large. Enhanced amplitude oscillations of the structures caused by galloping or flutter might result in substantial vibrations and therefore significant levels of captured power. However, due to its self-excitation and self-restriction, the VIV is less severe than flutter and galloping. Due to its small lock-in region, VIV energy conversion experiences large power swings as wind speeds fluctuate; this limits its applicability in environments with unpredictable vibration patterns. Flutter-based wind energy harvesting technology has advanced significantly, and new ideas and technologies have also been put forth recently. However, there are still several difficulties with flutter-based energy harvesting; for instance, these devices are unable to deliver stable output power at low wind speeds because of the existence of the cut-in wind speed. It might not be preferable for real-world applications due to the single structure's low energy harvesting efficiency. For the current challenges, researchers have put forth a variety of improvement techniques, including structural optimization, inducing nonlinearity and energy hybridization.

Considering the energy transduction mechanisms, the piezoelectric FBEHs are one of the most promising areas to extract energy from a wide range of fluid flows including wind and water, whereas comparatively, electromagnetic FBEHs are more suitable to gather energy from high-velocity fluid flows. Triboelectric energy harvesting has significant potential for advancing the development of self-powered sensors, wearable devices and other small-scale electronics, as well as contributing to the larger goal of harnessing renewable energy from ambient sources, such as wind and water wave energy. Despite significant advances and promising results in laboratories, the practical application of flow energy harvesting devices has encountered various challenges. The intricate nature of fluid dynamics and the variety of flow conditions in real environments are two of the key reasons why implementation has not kept pace with lab research. Flow energy harvesting systems rely primarily on the velocity and direction of the flow, which can vary drastically in real natural environments. As a result, maintaining the reliable and continuous generation of power from fluctuating flows remains a significant challenge that needs to be overcome in future. The key areas to be addressed in the field of flow-induced energy harvesting are to improve the efficiency, reliability and durability of FBEHs in harsh environments for long durations and increase the power density. This can be achieved by developing novel designs and advanced materials for FBEHs that are more efficient and inexpensive. As FBEH technology matures, it is projected to have a substantial impact on a variety of areas and applications. Some rotary wind energy harvesters (typically EM) are designed to harvest energy from several axes, allowing them to harvest wind energy with both rotational motion and induced vibrational motion along longitudinal, transverse or vertical directions. This feature broadens the range of potential energy sources that can be utilized. However, these solutions are only implemented and tested in a controlled laboratory environment, which may not accurately represent the complex and dynamic conditions of the real world.

Additionally, when energy is harvested, the power management circuit relies on various components, each of which requires power drawn from the harvester. In systems operating in variable wind conditions, efficiently distributing power to all components becomes particularly challenging, especially in compact designs where space and resources are limited. Furthermore, power circuits in remote regions are highly susceptible to failure due to harsh environmental conditions, inadequate infrastructure and the risk of physical damage. These factors can cause significant disruptions in the energy supply, complicating the reliable operation of the system.

To address the aforementioned problems, researchers should prioritize field testing and validation of FEHs in diverse and actual environments. Collaborations with industry partners can help to gain access to relevant testing grounds, ensuring that energy harvesters are resilient and effective under a variety of scenarios. Moreover, collaboration between academics and industry via establishing interdisciplinary research teams should be encouraged. By merging expertise in structural dynamics, flow-induced phe-

nomena, power management and wireless sensing, these teams can develop innovative solutions that address complex challenges. Creating collaborative research initiatives and industry–academic alliances and encouraging individuals with various experiences to collaborate can result in a more holistic approach to solving difficulties and producing comprehensive solutions.

10. Conclusions

Wind energy is widely recognized as one of the most cost-effective renewable energy sources, playing an important role in power conservation and the use of natural wind to power wireless sensor nodes. As a clean and sustainable energy alternative, it has grown in popularity in recent years, emerging as an important area of research in the development of self-powered sensing and monitoring systems. This work emphasizes wind energy harvesting and its ability to address rising energy demands while reducing environmental impact.

This review paper summarizes and classifies flow energy harvesters (FEHs)and as an examination of notable works in each direction of the development in FEHs, highlights the current state of the art. Numerous benefits and approaches for increasing energy harvesting capabilities are discussed, including how to handle recurrent issues in flow-induced vibration (FIV) energy harvesting. In FIV energy harvesting, the fluid–structure interaction, aerodynamic instabilities, structural dynamics and electromechanical coupling (transduction mechanism) are the important performance characteristics. Linear FEHs are limited by structural vulnerabilities and higher operational wind speed requirements, while nonlinear designs offer enhanced performance and durability.

Among transduction methods, piezoelectric and electromagnetic mechanisms are most suitable for their efficiency, scalability and ease of integration into various structures. Efficiency is significantly enhanced through the implementation of hybrid and coupled mechanisms, which leverage the strengths of multiple energy conversion methods and fluid dynamics interactions. Additionally, nonlinear energy harvesters have played a key role in enhancing output power by exploiting complex dynamic behaviors, enabling a broader frequency response and higher energy capture. These advancements contribute to more robust and efficient energy harvesting systems.

Along with the strengths and applications of FEHs, the paper also addresses limitations, such as vulnerabilities in structural design, power management challenges and energy conversion in remote areas. There is still a need for a general solution to model and design FIV energy harvesters. It is essential to focus on developing robust structural designs that can withstand environmental stresses and operational challenges. Implementing advanced power management systems will enhance energy distribution and optimize the performance of energy harvesters, particularly in diverse situations.

Furthermore, interdisciplinary collaboration between academia and industry is crucial for developing robust solutions. To synchronize technical requirements across multiple disciplines, researchers can pool their expertise, ensuring a comprehensive approach that addresses the complexities of each discipline and facilitates the seamless transition of wind energy harvesting concepts from theoretical realms to practical, real-world applications. Ultimately, these efforts will pave the way for more efficient, durable and adaptable wind energy harvesting systems, contributing to the sustainable utilization of wind energy for self-powered sensing and monitoring systems.

Author Contributions: Conceptualization, S.B., F.U.K., S.T. and A.Z.H.; formal analysis, S.B., F.U.K., A.Z.H., H.F. and S.T.; investigation, S.B., F.U.K., A.Z.H., H.F. and S.T.; writing—original draft preparation, S.B.; writing—review and editing, F.U.K., A.Z.H., H.F. and S.T.; supervision, S.T. and A.Z.H. All authors have read and agreed to the published version of the manuscript.

Funding: This research received no external funding.

Acknowledgments: This work has been supported by the Wolfson School of Mechanical, Electrical and Manufacturing Engineering, Loughborough University via the Overseas PhD Scholarship Scheme Phase-III, Higher Education Commission (Pakistan).

Conflicts of Interest: The authors declare no conflicts of interest.

References

1. Kuriakose, J.; Amruth, V.; Nandhini, N.S. A survey on localization of Wireless Sensor nodes. In Proceedings of the International Conference on Information Communication and Embedded Systems (ICICES2014), Chennai, India, 27–28 February 2015; pp. 6–11. [CrossRef]
2. Khalaf, O.I.; Sabbar, B.M. An overview on wireless sensor networks and finding optimal location of nodes. *Period. Eng. Nat. Sci.* **2019**, *7*, 1096–1101. [CrossRef]
3. Xu, C.; Song, Y.; Han, M.; Zhang, H. Portable and wearable self-powered systems based on emerging energy harvesting technology. *Microsyst. Nanoeng.* **2021**, *7*, 25. [CrossRef] [PubMed]
4. Bakhtiar, S.; Ilyas, M.; Khan, F.S.H.; Saadullah, C.; Viqar, M.Z.; Hussain, S.M.Z. *Flapping Induced Piezoelectric Transduction for Novel Disaster Management UAVs*; Springer Nature: Singapore, 2022; Volume 921. [CrossRef]
5. Masabi, S.N.; Fu, H.; Theodossiades, S. A bistable rotary-translational energy harvester from ultra-low-frequency motions for self-powered wireless sensing. *J. Phys. D Appl. Phys.* **2023**, *56*, 24001. [CrossRef]
6. Masabi, S.N.; Fu, H.; Flint, J.; Theodossiades, S. A multi-stable rotational energy harvester for arbitrary bi-directional horizontal excitation at ultra-low frequencies for self-powered sensing. *Smart Mater. Struct.* **2024**, *33*, 95017. [CrossRef]
7. Izhar; Khan, F.U. Electromagnetic based acoustic energy harvester for low power wireless autonomous sensor applications. *Sens. Rev.* **2018**, *38*, 298–310. [CrossRef]
8. Zhang, Y.; Xie, M.; Adamaki, V.; Khanbareh, H.; Bowen, C.R. Control of electro-chemical processes using energy harvesting materials and devices. *Chem. Soc. Rev.* **2017**, *46*, 7757–7786. [CrossRef]
9. Tao, J.X.; Viet, N.V.; Carpinteri, A.; Wang, Q. Energy harvesting from wind by a piezoelectric harvester. *Eng. Struct.* **2017**, *133*, 74–80. [CrossRef]
10. Cuadras, A.; Gasulla, M.; Ferrari, V. Thermal energy harvesting through pyroelectricity. *Sens. Actuators A Phys.* **2010**, *158*, 132–139. [CrossRef]
11. Khan, A.S.; Khan, F.U. A Wearable Solar Energy Harvesting Based Jacket With Maximum Power Point Tracking for Vital Health Monitoring Systems. *IEEE Access* **2022**, *10*, 119475–119495. [CrossRef]
12. Kim, M.; Dugundji, J.; Wardle, B.L. Efficiency of piezoelectric mechanical vibration energy harvesting. *Smart Mater. Struct.* **2015**, *24*, 055006. [CrossRef]
13. Bowen, C.R.; Taylor, J.; Leboulbar, E.; Zabek, D.; Chauhan, A.; Vaish, R. Pyroelectric materials and devices for energy harvesting applications. *Energy Environ. Sci.* **2014**, *7*, 3836–3856. [CrossRef]
14. Zou, H.-X.; Zhao, L.-C.; Wang, Q.; Gao, Q.-H.; Yan, G.; Wei, K.-X.; Zhang, W.-M. A self-regulation strategy for triboelectric nanogenerator and self-powered wind-speed sensor. *Nano Energy* **2022**, *95*, 106990. [CrossRef]
15. Wang, J.; Yurchenko, D.; Hu, G.; Zhao, L.; Tang, L.; Yang, Y. Perspectives in flow-induced vibration energy harvesting. *Appl. Phys. Lett.* **2021**, *119*, 100502. [CrossRef]
16. Parameshwaran, R.; Dhulipalla, S.J.; Yendluri, D.R. Fluid-structure Interactions and Flow Induced Vibrations: A Review. *Procedia Eng.* **2016**, *144*, 1286–1293. [CrossRef]
17. Nishi, Y.; Fukuda, K.; Shinohara, W. Experimental energy harvesting from fluid flow by using two vibrating masses. *J. Sound Vib.* **2017**, *394*, 321–332. [CrossRef]
18. Zou, H.X.; Li, M.; Zhao, L.C.; Gao, Q.H.; Wei, K.X.; Zuo, L.; Qian, F.; Zhang, W.M. A magnetically coupled bistable piezoelectric harvester for underwater energy harvesting. *Energy* **2021**, *217*, 119429. [CrossRef]
19. Mehmood, A.; Abdelkefi, A.; Hajj, M.R.; Nayfeh, A.H.; Akhtar, I.; Nuhait, A.O. Piezoelectric energy harvesting from vortex-induced vibrations of circular cylinder. *J. Sound Vib.* **2013**, *332*, 4656–4667. [CrossRef]
20. McCarthy, J.M.; Watkins, S.; Deivasigamani, A.; John, S.J. Fluttering energy harvesters in the wind: A review. *J. Sound Vib.* **2016**, *361*, 355–377. [CrossRef]
21. Yan, Z.; Abdelkefi, A.; Hajj, M.R. Piezoelectric energy harvesting from hybrid vibrations. *Smart Mater. Struct.* **2014**, *23*, 025026. [CrossRef]
22. Abdelkefi, A.; Scanlon, J.M.; McDowell, E.; Hajj, M.R. Performance enhancement of piezoelectric energy harvesters from wake galloping. *Appl. Phys. Lett.* **2013**, *103*, 033903. [CrossRef]
23. Hobeck, J.D.; Inman, D.J. Energy Harvesting From Turbulence-Induced Vibration in Air Flow: Artificial Piezoelectric Grass Concept. In Proceedings of the ASME 2011 Conference on Smart Materials, Adaptive Structures and Intelligent Systems, Scottsdale, AZ, USA, 18–21 September 2011; pp. 637–646. [CrossRef]
24. Bakhtiar, S.; Khan, F.U.; Rahman, W.U.; Khan, A.S.; Ahmad, M.M.; Iqbal, M. A Pressure-Based Electromagnetic Energy Harvester for Pipeline Monitoring Applications. *J. Sens.* **2022**, *2022*, 6529623. [CrossRef]

25. Bakhtiar, S.; Hajjaj, A.Z.; Fu, H.; Theodossiades, S. A Two-Body Low-Frequency Piezoelectric Wind Energy Harvester for Environmental Sensing. In Proceedings of the IEMTRONICS 2024, International IOT, Electronics and Mechatronics Conference, London, UK, 3–5 April 2024; pp. 5–11.
26. Barrero-Gil, A.; Alonso, G.; Sanz-Andres, A. Energy harvesting from transverse galloping. *J. Sound Vib.* **2010**, *329*, 2873–2883. [CrossRef]
27. Khan, F.U.; Ahmad, S. Flow type electromagnetic based energy harvester for pipeline health monitoring system. *Energy Convers. Manag.* **2019**, *200*, 112089. [CrossRef]
28. Bakhtiar, S.; Khan, F.U. Energy harvesting from pulsating fluid flow for pipeline monitoring systems. In Proceedings of the 2019 International Symposium on Recent Advances in Electrical Engineering (RAEE), Islamabad, Pakistan, 28–29 August 2019; Volume 4, pp. 1–6. [CrossRef]
29. Lee, G.; Lee, D.; Park, J.; Jang, Y.; Kim, M.; Rho, J. Piezoelectric energy harvesting using mechanical metamaterials and phononic crystals. *Commun. Phys.* **2022**, *5*, 94. [CrossRef]
30. Zargari, S.; Daie Koozehkanani, Z.; Veladi, H.; Sobhi, J.; Rezania, A. A new Mylar-based triboelectric energy harvester with an innovative design for mechanical energy harvesting applications. *Energy Convers. Manag.* **2021**, *244*, 114489. [CrossRef]
31. Hou, C.; Li, C.; Shan, X.; Yang, C.; Song, R.; Xie, T. A broadband piezo-electromagnetic hybrid energy harvester under combined vortex-induced and base excitations. *Mech. Syst. Signal Process.* **2022**, *171*, 108963. [CrossRef]
32. Anton, S.R.; Sodano, H.A. A review of power harvesting using piezoelectric materials (2003–2006). *Smart Mater. Struct.* **2007**, *16*, R1. [CrossRef]
33. Ng, T.H.; Liao, W.H. Sensitivity analysis and energy harvesting for a self-powered piezoelectric sensor. *J. Intell. Mater. Syst. Struct.* **2005**, *16*, 785–797. [CrossRef]
34. Yang, B.; Lee, C.; Xiang, W.; Xie, J.; He, J.H.; Kotlanka, R.K.; Low, S.P.; Feng, H. Electromagnetic energy harvesting from vibrations of multiple frequencies. *J. Micromech. Microeng.* **2009**, *19*, 35001. [CrossRef]
35. Li, P.; Wen, Y.; Liu, P.; Li, X.; Jia, C. A magnetoelectric energy harvester and management circuit for wireless sensor network. *Sens. Actuators A Phys.* **2010**, *157*, 100–106. [CrossRef]
36. Foisal, A.R.M.; Hong, C.; Chung, G.S. Multi-frequency electromagnetic energy harvester using a magnetic spring cantilever. *Sens. Actuators A Phys.* **2012**, *182*, 106–113. [CrossRef]
37. Lin, Z.; Chen, J.; Yang, J. Recent Progress in Triboelectric Nanogenerators as a Renewable and Sustainable Power Source. *J. Nanomater.* **2016**, *2016*, 5651613. [CrossRef]
38. Zou, Y.; Raveendran, V.; Chen, J. Wearable triboelectric nanogenerators for biomechanical energy harvesting. *Nano Energy* **2020**, *77*, 105303. [CrossRef]
39. Wang, D.-A.; Pham, H.-T.; Chao, C.-W.; Chen, J.M. A Piezoelectric Energy Harvester Based on Pressure Fluctuations in Karman Vortex Street. In Proceedings of the World Renewable Energy Congress, Sweden, Linköping, Sweden, 8–13 May 2011; Volume 57, pp. 1456–1463. [CrossRef]
40. Païdoussis, M.P.; Price, S.J.; De Langre, E. *Fluid-Structure Interactions: Cross-Flow-Induced Instabilities*; Cambridge University Press: Cambridge, UK, 2011.
41. Akaydin, H.D.; Elvin, N.; Andreopoulos, Y. Energy harvesting from highly unsteady fluid flows using piezoelectric materials. *J. Intell. Mater. Syst. Struct.* **2010**, *21*, 1263–1278. [CrossRef]
42. Song, R.; Shan, X.; Lv, F.; Xie, T. A study of vortex-induced energy harvesting from water using PZT piezoelectric cantilever with cylindrical extension. *Ceram. Int.* **2015**, *41*, S768–S773. [CrossRef]
43. Demori, M.; Ferrari, M.; Bonzanini, A.; Poesio, P.; Ferrari, V. Autonomous sensors powered by energy harvesting from von Karman vortices in airflow. *Sensors* **2017**, *17*, 2100. [CrossRef]
44. Thein, C.K.; Liu, J.-S. Numerical modeling of shape and topology optimisation of a piezoelectric cantilever beam in an energy-harvesting sensor. *Eng. Comput.* **2017**, *33*, 137–148. [CrossRef]
45. Ding, L.; Zhang, L.; Wu, C.; Mao, X.; Jiang, D. Flow induced motion and energy harvesting of bluff bodies with different cross sections. *Energy Convers. Manag.* **2015**, *91*, 416–426. [CrossRef]
46. Kan, J.; Liao, W.; Wang, J.; Wang, S.; Yan, M.; Jiang, Y.; Zhang, Z. Enhanced piezoelectric wind-induced vibration energy harvester via the interplay between cylindrical shell and diamond-shaped baffle. *Nano Energy* **2021**, *89*, 106466. [CrossRef]
47. Gong, Y.; Shan, X.; Luo, X.; Pan, J.; Xie, T.; Yang, Z. Direction-adaptive energy harvesting with a guide wing under flow-induced oscillations. *Energy* **2019**, *187*, 115983. [CrossRef]
48. Hu, Y.; Yang, B.; Chen, X.; Wang, X.; Liu, J. Modeling and experimental study of a piezoelectric energy harvester from vortex shedding-induced vibration. *Energy Convers. Manag.* **2018**, *162*, 145–158. [CrossRef]
49. Du, X.; Zhang, M.; Chang, H.; Wang, Y.; Yu, H. Micro windmill piezoelectric energy harvester based on vortex-induced vibration in tunnel. *Energy* **2022**, *238*, 121734. [CrossRef]
50. Zuo, L.; Tang, X. Large-scale vibration energy harvesting. *J. Intell. Mater. Syst. Struct.* **2013**, *24*, 1405–1430. [CrossRef]
51. Gong, Y.; Yang, Z.; Shan, X.; Sun, Y.; Xie, T.; Zi, Y. Capturing Flow Energy from Ocean and Wind. *Energies* **2019**, *12*, 2184. [CrossRef]
52. Xie, X.D.; Wang, Q.; Wu, N. Energy harvesting from transverse ocean waves by a piezoelectric plate. *Int. J. Eng. Sci.* **2014**, *81*, 41–48. [CrossRef]

53. Dai, H.L.; Abdelkefi, A.; Yang, Y.; Wang, L. Orientation of bluff body for designing efficient energy harvesters from vortex-induced vibrations. *Appl. Phys. Lett.* **2016**, *108*, 53902. [CrossRef]
54. Zhou, G.; Li, Z.; Zhu, Z.; Hao, B.; Tang, C. A New Piezoelectric Bimorph Energy Harvester Based on the Vortex-Induced-Vibration Applied in Rotational Machinery. *IEEE/ASME Trans. Mechatron.* **2019**, *24*, 700–709. [CrossRef]
55. Wang, M.; Wang, W.; Li, Q. Structural optimization of laminated leaf-like piezoelectric wind energy harvesters based on topological method. *Adv. Mech. Eng.* **2024**, *16*, 16878132231224577. [CrossRef]
56. Wang, D.-A.; Chang, K.-H. Electromagnetic energy harvesting from flow induced vibration. *Microelectron. J.* **2010**, *41*, 356–364. [CrossRef]
57. Wang, D.A.; Chiu, C.Y.; Pham, H.T. Electromagnetic energy harvesting from vibrations induced by Kármán vortex street. *Mechatronics* **2012**, *22*, 746–756. [CrossRef]
58. Sarviha, A.; Barati, E.; Zarkak, M.R.; Derakhshandeh, J.F.; Alam, M.M. Experimental Investigations on the Wake-Induced Vibration of an Electromagnetic Energy-Harvesting System. *Int. J. Energy Res.* **2024**, *2024*, 7072340. [CrossRef]
59. Zhang, L.; Meng, B.; Tian, Y.; Meng, X.; Lin, X.; He, Y.; Xing, C.; Dai, H.; Wang, L. Vortex-induced vibration triboelectric nanogenerator for low speed wind energy harvesting. *Nano Energy* **2022**, *95*, 107029. [CrossRef]
60. Wang, Y.; Chen, T.; Sun, S.; Liu, X.; Hu, Z.; Lian, Z.; Liu, L.; Shi, Q.; Wang, H.; Mi, J.; et al. A humidity resistant and high performance triboelectric nanogenerator enabled by vortex-induced vibration for scavenging wind energy. *Nano Res.* **2022**, *15*, 3246–3253. [CrossRef]
61. Li, X.; Zhou, Y.; Li, Z.; Guo, H.; Gong, Y.; Zhang, D.; Zhang, D.; Zhang, Q.; Wang, B.; Peng, Y. Vortex-induced vibration triboelectric nanogenerator for energy harvesting from low-frequency water flow. *Energy Convers. Manag.* **2023**, *292*, 117383. [CrossRef]
62. Han, Y.; Wu, F.; Du, X.; Li, Z.; Chen, H.; Guo, D.; Wang, J.; Yu, H. Enhance vortices vibration with Y-type bluff body to decrease arousing wind speed and extend range for flag triboelectric energy harvester. *Nano Energy* **2024**, *119*, 109063. [CrossRef]
63. Choi, J.-A.; Jeong, J.; Kang, M.; Ko, H.-J.; Kim, T.; Park, K.; Kim, J.; Pyo, S. Externally motionless triboelectric nanogenerator based on vortex-induced rolling for omnidirectional wind energy harvesting. *Nano Energy* **2024**, *119*, 109071. [CrossRef]
64. Bashir, M.; Rajendran, P.; Khan, S.A. Energy Harvesting from Aerodynamic Instabilities: Current prospect and Future Trends. *IOP Conf. Ser. Mater. Sci. Eng.* **2018**, *290*, 012054. [CrossRef]
65. Yang, Y.; Zhao, L.; Tang, L. Comparative study of tip cross-sections for efficient galloping energy harvesting. *Appl. Phys. Lett.* **2013**, *102*, 064105. [CrossRef]
66. Sirohi, J.; Mahadik, R. Piezoelectric wind energy harvester for low-power sensors. *J. Intell. Mater. Syst. Struct.* **2011**, *22*, 2215–2228. [CrossRef]
67. Sirohi, J.; Mahadik, R. Harvesting wind energy using a galloping piezoelectric beam. *J. Vib. Acoust. Trans. ASME* **2012**, *134*, 011009. [CrossRef]
68. Abdelkefi, A.; Hajj, M.R.; Nayfeh, A.H. Piezoelectric energy harvesting from transverse galloping of bluff bodies. *Smart Mater. Struct.* **2013**, *22*, 015014. [CrossRef]
69. Zhao, L.; Tang, L.; Yang, Y. Comparison of modeling methods and parametric study for a piezoelectric wind energy harvester. *Smart Mater. Struct.* **2013**, *22*, 125003. [CrossRef]
70. Hémon, P.; Amandolese, X.; Andrianne, T. Energy harvesting from galloping of prisms: A wind tunnel experiment. *J. Fluids Struct.* **2017**, *70*, 390–402. [CrossRef]
71. Bibo, A.; Daqaq, M.F. On the optimal performance and universal design curves of galloping energy harvesters. *Appl. Phys. Lett.* **2014**, *104*, 023901. [CrossRef]
72. Hu, G.; Tse, K.T.; Kwok, K.C.S.; Song, J.; Lyu, Y. Aerodynamic modification to a circular cylinder to enhance the piezoelectric wind energy harvesting. *Appl. Phys. Lett.* **2016**, *109*, 193902. [CrossRef]
73. Hu, G.; Tse, K.T.; Kwok, K.C.S. Enhanced performance of wind energy harvester by aerodynamic treatment of a square prism. *Appl. Phys. Lett.* **2016**, *108*, 123901. [CrossRef]
74. Liu, F.R.; Zou, H.X.; Zhang, W.M.; Peng, Z.K.; Meng, G. Y-type three-blade bluff body for wind energy harvesting. *Appl. Phys. Lett.* **2018**, *112*, 233903. [CrossRef]
75. Liu, F.R.; Zhang, W.M.; Peng, Z.K.; Meng, G. Fork-shaped bluff body for enhancing the performance of galloping-based wind energy harvester. *Energy* **2019**, *183*, 92–105. [CrossRef]
76. Wang, J.; Zhou, S.; Zhang, Z.; Yurchenko, D. High-performance piezoelectric wind energy harvester with Y-shaped attachments. *Energy Convers. Manag.* **2019**, *181*, 645–652. [CrossRef]
77. Sun, W.; Jo, S.; Seok, J. Development of the optimal bluff body for wind energy harvesting using the synergetic effect of coupled vortex induced vibration and galloping phenomena. *Int. J. Mech. Sci.* **2019**, *156*, 435–445. [CrossRef]
78. Zhou, C.F.; Zou, H.X.; Wei, K.X.; Liu, J.G. Enhanced performance of piezoelectric wind energy harvester by a curved plate. *Smart Mater. Struct.* **2019**, *28*, 125022. [CrossRef]
79. Tucker Harvey, S.; Khovanov, I.A.; Denissenko, P. A galloping energy harvester with flow attachment. *Appl. Phys. Lett.* **2019**, *114*, 104103. [CrossRef]
80. Noel, J.; Yadav, R.; Li, G.; Daqaq, M.F. Improving the performance of galloping micro-power generators by passively manipulating the trailing edge. *Appl. Phys. Lett.* **2018**, *112*, 83503. [CrossRef]
81. Jo, S.; Sun, W.; Son, C.; Seok, J. Galloping-based energy harvester considering enclosure effect. *AIP Adv.* **2018**, *8*, 095309. [CrossRef]

82. Zhao, K.; Zhang, Q.; Wang, W. Optimization of galloping piezoelectric energy harvester with V-shaped groove in low wind speed. *Energies* **2019**, *12*, 4619. [CrossRef]
83. Siriyothai, P.; Kittichaikarn, C. Performance enhancement of a galloping-based energy harvester with different groove depths on square bluff body. *Renew. Energy* **2023**, *210*, 148–158. [CrossRef]
84. Wang, W.; Huang, J.; Yao, Z. Cut-corner prism piezoelectric energy harvester based on galloping enhancement mechanism. *Energy Rep.* **2021**, *7*, 6366–6374. [CrossRef]
85. Zhao, D.; Hu, X.; Tan, T.; Yan, Z.; Zhang, W. Piezoelectric galloping energy harvesting enhanced by topological equivalent aerodynamic design. *Energy Convers. Manag.* **2020**, *222*, 113260. [CrossRef]
86. Yuan, Y.; Wang, H.; Yang, C.; Sun, H.; Tang, Y.; Zhang, Z. Exploring the Potential of Flow-Induced Vibration Energy Harvesting Using a Corrugated Hyperstructure Bluff Body. *Micromachines* **2023**, *14*, 1125. [CrossRef]
87. Wang, J.; Kan, J.; Gu, Y.; He, C.; Ren, Z.; Meng, F.; Wang, S.; Zhang, Z. Design, performance evaluation and calibration of an indirectly-excited piezoelectric wind energy harvester via a double-bluffbody exciter. *Energy Convers. Manag.* **2023**, *284*, 116969. [CrossRef]
88. Liu, J.; Bao, B.; Chen, J.; Wu, Y.; Wang, Q. Passively adaptive wind energy harvester featuring a double-airfoil bluff body with adjustable attack angles. *Mech. Syst. Signal Process.* **2023**, *185*, 109814. [CrossRef]
89. Tan, T.; Zuo, L.; Yan, Z. Environment coupled piezoelectric galloping wind energy harvesting. *Sens. Actuators A Phys.* **2021**, *323*, 112641. [CrossRef]
90. Hu, S.; Zhao, D.; Sun, W.; Liu, Y.; Ma, C. Investigation on galloping piezoelectric energy harvester considering the surface roughness in low velocity water flow. *Energy* **2023**, *262*, 125478. [CrossRef]
91. Xia, C.; Yang, J.; Tang, L.; Yin, P.; Li, Z.; Wang, B.; Aw, K.C. A multi-directional and multi-modal galloping piezoelectric energy harvester with tri-section beam. *Smart Mater. Struct.* **2024**, *33*, 035045. [CrossRef]
92. Ali, M.; Arafa, M.; Elaraby, M. Harvesting energy from galloping oscillations. *Lect. Notes Eng. Comput. Sci.* **2013**, *3*, 2053–2058.
93. Zhang, L.B.; Dai, H.L.; Abdelkefi, A.; Lin, S.X.; Wang, L. Theoretical modeling, wind tunnel measurements, and realistic environment testing of galloping-based electromagnetic energy harvesters. *Appl. Energy* **2019**, *254*, 113737. [CrossRef]
94. Xiong, L.; Gao, S.; Jin, L.; Guo, S.; Sun, Y.; Liu, F. The Design and Experiment of a Spring-Coupling Electromagnetic Galloping Energy Harvester. *Micromachines* **2023**, *14*, 968. [CrossRef]
95. Kim, H.; Kim, S.; Xue, K.; Seok, J. Modeling and performance analysis of electromagnetic energy harvester based on torsional galloping phenomenon. *Mech. Syst. Signal Process.* **2023**, *195*, 110287. [CrossRef]
96. Su, B.; Wang, Y.; Li, J.; Guo, T.; Cheng, G.; Sun, W. A novel elastic strip suspension-based bi-directional electromagnetic wind energy harvester designed specifically for wind energy factories. *Mech. Syst. Signal Process.* **2024**, *208*, 111059. [CrossRef]
97. Zhang, L.; Meng, B.; Xia, Y.; Deng, Z.; Dai, H.; Hagedorn, P.; Peng, Z.; Wang, L. Galloping triboelectric nanogenerator for energy harvesting under low wind speed. *Nano Energy* **2020**, *70*, 104477. [CrossRef]
98. Zeng, Q.; Wu, Y.; Tang, Q.; Liu, W.; Wu, J.; Zhang, Y.; Yin, G.; Yang, H.; Yuan, S.; Tan, D.; et al. A high-efficient breeze energy harvester utilizing a full-packaged triboelectric nanogenerator based on flow-induced vibration. *Nano Energy* **2020**, *70*, 104524. [CrossRef]
99. Zhang, S.; Jing, Z.; Wang, X.; Zhu, M.; Yu, X.; Zhu, J.; Cheng, T.; Zhao, H.; Wang, Z.L. Soft-bionic-fishtail structured triboelectric nanogenerator driven by flow-induced vibration for low-velocity water flow energy harvesting. *Nano Res.* **2023**, *16*, 466–472. [CrossRef]
100. Cao, L.N.Y.; Su, E.; Xu, Z.; Wang, Z.L. Fully enclosed microbeads structured TENG arrays for omnidirectional wind energy harvesting with a portable galloping oscillator. *Mater. Today* **2023**, *71*, 9–21. [CrossRef]
101. Ma, X.; Zhou, S. A review of flow-induced vibration energy harvesters. *Energy Convers. Manag.* **2022**, *254*, 115223. [CrossRef]
102. Wen, Q.; He, X.; Lu, Z.; Streiter, R.; Otto, T. A comprehensive review of miniatured wind energy harvesters. *Nano Mater. Sci.* **2021**, *3*, 170–185. [CrossRef]
103. Ravi, S.; Zilian, A. Simultaneous finite element analysis of circuit-integrated piezoelectric energy harvesting from fluid-structure interaction. *Mech. Syst. Signal Process.* **2019**, *114*, 259–274. [CrossRef]
104. Erturk, A.; Bilgen, O.; Fontenille, M.; Inman, D.J. Piezoelectric energy harvesting from macro-fiber composites with an application to morphing-wing aircrafts. In Proceedings of the 19th International Conference on Adaptive Structures and Technologies 2008 (ICAST 2008), Ascona, Switzerland, 6–9 October 2008; pp. 339–359.
105. Erturk, A.; Vieira, W.G.R.; De Marqui, C.; Inman, D.J. On the energy harvesting potential of piezoaeroelastic systems. *Appl. Phys. Lett.* **2010**, *96*, 184103. [CrossRef]
106. Bryant, M.; Garcia, E. Modeling and Testing of a Novel Aeroelastic Flutter Energy Harvester. *J. Vib. Acoust.* **2011**, *133*, 011010. [CrossRef]
107. Kwon, S.D. A T-shaped piezoelectric cantilever for fluid energy harvesting. *Appl. Phys. Lett.* **2010**, *97*, 164102. [CrossRef]
108. Bibo, A.; Daqaq, M.F. Investigation of concurrent energy harvesting from ambient vibrations and wind using a single piezoelectric generator. *Appl. Phys. Lett.* **2013**, *102*, 243904. [CrossRef]
109. Zakaria, M.Y.; Al-Haik, M.Y.; Hajj, M.R. Experimental analysis of energy harvesting from self-induced flutter of a composite beam. *Appl. Phys. Lett.* **2015**, *107*, 2–6. [CrossRef]
110. Eugeni, M.; Elahi, H.; Fune, F.; Lampani, L.; Mastroddi, F.; Romano, G.P.; Gaudenzi, P. Numerical and experimental investigation of piezoelectric energy harvester based on flag-flutter. *Aerosp. Sci. Technol.* **2020**, *97*, 105634. [CrossRef]

111. Agarwal, A.; Purohit, A. On the performance improvement of a flutter based energy harvester by introducing additional wake field. In *Energy Sources, Part A: Recovery, Utilization, and Environmental Effects*; Taylor & Francis: Oxfordshire, UK, 2021; pp. 1–14. [CrossRef]
112. Latif, U.; Dowell, E.H.; Uddin, E.; Yamin Younis, M. Parametric aerodynamic and aeroelastic study of a deformable flag-based energy harvester for powering low energy devices. *Energy Convers. Manag.* **2023**, *280*, 116846. [CrossRef]
113. Zhu, D.; Beeby, S.; Tudor, J.; White, N.; Harris, N. A novel miniature wind generator for wireless sensing applications. *Proc. IEEE Sens.* **2010**, *1*, 1415–1418. [CrossRef]
114. Park, J.; Morgenthal, G.; Kim, K.; Kwon, S.D.; Law, K.H. Power evaluation of flutter-based electromagnetic energy harvesters using computational fluid dynamics simulations. *J. Intell. Mater. Syst. Struct.* **2014**, *25*, 1800–1812. [CrossRef]
115. Dinh Quy, V.; Van Sy, N.; Tan Hung, D.; Quoc Huy, V. Wind tunnel and initial field tests of a micro generator powered by fluid-induced flutter. *Energy Sustain. Dev.* **2016**, *33*, 75–83. [CrossRef]
116. Atrah, A.B.; Ab-Rahman, M.S.; Salleh, H.; Nuawi, M.Z.; Mohd Nor, M.J.; Jamaludin, N. Bin Karman Vortex Creation Using Cylinder for Flutter Energy Harvester Device. *Micromachines* **2017**, *8*, 227. [CrossRef]
117. Lu, Z.; Wen, Q.; He, X.; Wen, Z. A Flutter-Based Electromagnetic Wind Energy Harvester: Theory and Experiments. *Appl. Sci.* **2019**, *9*, 4823. [CrossRef]
118. Nabavi, S.; Zhang, L. Portable wind energy harvesters for low-power applications: A survey. *Sensors* **2016**, *16*, 1101. [CrossRef]
119. Zhao, Z.; Pu, X.; Du, C.; Li, L.; Jiang, C.; Hu, W.; Wang, Z.L. Freestanding Flag-Type Triboelectric Nanogenerator for Harvesting High-Altitude Wind Energy from Arbitrary Directions. *ACS Nano* **2016**, *10*, 1780–1787. [CrossRef]
120. Phan, H.; Shin, D.-M.; Heon Jeon, S.; Young Kang, T.; Han, P.; Han Kim, G.; Kook Kim, H.; Kim, K.; Hwang, Y.-H.; Won Hong, S. Aerodynamic and aeroelastic flutters driven triboelectric nanogenerators for harvesting broadband airflow energy. *Nano Energy* **2017**, *33*, 476–484. [CrossRef]
121. Liu, X.; Zhao, K.; Yang, Y. Effective polarization of ferroelectric materials by using a triboelectric nanogenerator to scavenge wind energy. *Nano Energy* **2018**, *53*, 622–629. [CrossRef]
122. Lin, H.; He, M.; Jing, Q.; Yang, W.; Wang, S.; Liu, Y.; Zhang, Y.; Li, J.; Li, N.; Ma, Y.; et al. Angle-shaped triboelectric nanogenerator for harvesting environmental wind energy. *Nano Energy* **2019**, *56*, 269–276. [CrossRef]
123. Feng, Y.; Zhang, L.; Zheng, Y.; Wang, D.; Zhou, F.; Liu, W. Leaves based triboelectric nanogenerator (TENG) and TENG tree for wind energy harvesting. *Nano Energy* **2019**, *55*, 260–268. [CrossRef]
124. Ravichandran, A.N.; Calmes, C.; Serres, J.R.; Ramuz, M.; Blayac, S. Compact and high performance wind actuated venturi triboelectric energy harvester. *Nano Energy* **2019**, *62*, 449–457. [CrossRef]
125. Wang, Y.; Yang, E.; Chen, T.; Wang, J.; Hu, Z.; Mi, J.; Pan, X.; Xu, M. A novel humidity resisting and wind direction adapting flag-type triboelectric nanogenerator for wind energy harvesting and speed sensing. *Nano Energy* **2020**, *78*, 105279. [CrossRef]
126. Gao, S.; Zeng, X.; Chen, X.; Liao, T.; Wang, R.; Chen, Y.; Wei, H.; Luo, X.; Feng, S. Self-powered system for environment and aeolian vibration monitoring in the high-voltage transmission system by multi-directional wind-driven triboelectric nanogenerator. *Nano Energy* **2023**, *117*, 108911. [CrossRef]
127. Tadrist, L.; Julio, K.; Saudreau, M.; de Langre, E. Leaf flutter by torsional galloping: Experiments and model. *J. Fluids Struct.* **2015**, *56*, 1–10. [CrossRef]
128. Li, S.; Yuan, J.; Lipson, H. Ambient wind energy harvesting using cross-flow fluttering. *J. Appl. Phys.* **2011**, *109*, 26104. [CrossRef]
129. Hobbs, W.B.; Hu, D.L. Tree-inspired piezoelectric energy harvesting. *J. Fluids Struct.* **2012**, *28*, 103–114. [CrossRef]
130. Ahmed, A.; Hassan, I.; Song, P.; Gamaleldin, M.; Radhi, A.; Panwar, N.; Tjin, S.C.; Desoky, A.Y.; Sinton, D.; Yong, K.-T.; et al. Self-adaptive Bioinspired Hummingbird-wing Stimulated Triboelectric Nanogenerators. *Sci. Rep.* **2017**, *7*, 17143. [CrossRef] [PubMed]
131. Bo, F.; Jiwen, F.; Jiuchun, Z.; Chong, L.; Jia, W.; Mingming, L. Bionic flutter wing piezoelectric-electromagnetic composite energy harvesting system. *Energy Convers. Manag.* **2022**, *271*, 116319. [CrossRef]
132. Al-Haik, M.Y.; Kabir, M.M.; Siddique, W.; AlNuaimi, S.; Aldajah, S. An experimental study on piezoelectric energy harvesting from palm tree induced by wind. *Eng. Res. Express* **2020**, *2*, 25044. [CrossRef]
133. Liu, J.; Zuo, H.; Xia, W.; Luo, Y.; Yao, D.; Chen, Y.; Wang, K.; Li, Q. Wind energy harvesting using piezoelectric macro fiber composites based on flutter mode. *Microelectron. Eng.* **2020**, *231*, 111333. [CrossRef]
134. Wang, K.; Xia, W.; Lin, T.; Wu, J.; Hu, S. Low-speed flutter of artificial stalk-leaf and its application in wind energy harvesting. *Smart Mater. Struct.* **2021**, *30*, 125002. [CrossRef]
135. Wang, K.; Xia, W.; Ren, J.; Yu, W.; Feng, H.; Hu, S. Wind energy harvesting inspired by Palm leaf flutter: Observation, mechanism and experiment. *Energy Convers. Manag.* **2023**, *284*, 116971. [CrossRef]
136. Alhadidi, A.H.; Abderrahmane, H.; Daqaq, M.F. Exploiting stiffness nonlinearities to improve flow energy capture from the wake of a bluff body. *Phys. D Nonlinear Phenom.* **2016**, *337*, 30–42. [CrossRef]
137. Zhang, B.; Song, B.; Mao, Z.; Tian, W.; Li, B. Numerical investigation on VIV energy harvesting of bluff bodies with different cross sections in tandem arrangement. *Energy* **2017**, *133*, 723–736. [CrossRef]
138. Sun, H.; Ma, C.; Kim, E.S.; Nowakowski, G.; Mauer, E.; Bernitsas, M.M. Hydrokinetic energy conversion by two rough tandem-cylinders in flow induced motions: Effect of spacing and stiffness. *Renew. Energy* **2017**, *107*, 61–80. [CrossRef]
139. Usman, M.; Hanif, A.; Kim, I.H.; Jung, H.J. Experimental validation of a novel piezoelectric energy harvesting system employing wake galloping phenomenon for a broad wind spectrum. *Energy* **2018**, *153*, 882–889. [CrossRef]

140. AkaydIn, H.D.; Elvin, N.; Andreopoulos, Y. Wake of a cylinder: A paradigm for energy harvesting with piezoelectric materials. *Exp. Fluids* **2010**, *49*, 291–304. [CrossRef]
141. Jung, H.J.; Lee, S.W. The experimental validation of a new energy harvesting system based on the wake galloping phenomenon. *Smart Mater. Struct.* **2011**, *20*, 055022. [CrossRef]
142. Sivadas, V.; Wickenheiser, A.M. A study of several vortex-induced vibration techniques for piezoelectric wind energy harvesting. *Act. Passiv. Smart Struct. Integr. Syst.* **2011**, *7977*, 79770F. [CrossRef]
143. Uttayopas, P.; Kittichaikarn, C. Effects of downstream structures on aero elastic energy harvesters from wake-induced vibration. *J. Fluids Eng. Trans. ASME* **2019**, *141*, 071103. [CrossRef]
144. Zhang, L.B.; Dai, H.L.; Abdelkefi, A.; Wang, L. Experimental investigation of aerodynamic energy harvester with different interference cylinder cross-sections. *Energy* **2019**, *167*, 970–981. [CrossRef]
145. Shan, X.; Li, H.; Yang, Y.; Feng, J.; Wang, Y.; Xie, T. Enhancing the performance of an underwater piezoelectric energy harvester based on flow-induced vibration. *Energy* **2019**, *172*, 134–140. [CrossRef]
146. Yan, Z.; Wang, L.; Hajj, M.R.; Yan, Z.; Sun, Y.; Tan, T. Energy harvesting from iced-conductor inspired wake galloping. *Extrem. Mech. Lett.* **2020**, *35*, 100633. [CrossRef]
147. Kim, H.; Lee, J.; Seok, J. Novel piezoelectric wind energy harvester based on coupled galloping phenomena with characterization and quantification of its dynamic behavior. *Energy Convers. Manag.* **2022**, *266*, 115849. [CrossRef]
148. Yuan, S.; Zeng, Q.; Tan, D.; Luo, Y.; Zhang, X.; Guo, H.; Wang, X.; Wang, Z.L. Scavenging breeze wind energy (1–8.1 ms^{-1}) by minimalist triboelectric nanogenerator based on the wake galloping phenomenon. *Nano Energy* **2022**, *100*, 107465. [CrossRef]
149. Wang, J.; Geng, L.; Ding, L.; Zhu, H.; Yurchenko, D. The state-of-the-art review on energy harvesting from flow-induced vibrations. *Appl. Energy* **2020**, *267*, 114902. [CrossRef]
150. Mackowski, A.W.; Williamson, C.H.K. An experimental investigation of vortex-induced vibration with nonlinear restoring forces. *Phys. Fluids* **2013**, *25*, 087101. [CrossRef]
151. Dai, H.L.; Abdelkefi, A.; Wang, L. Theoretical modeling and nonlinear analysis of piezoelectric energy harvesting from vortex-induced vibrations. *J. Intell. Mater. Syst. Struct.* **2014**, *25*, 1861–1874. [CrossRef]
152. Zhang, J.; Zhang, J.; Shu, C.; Fang, Z. Enhanced piezoelectric wind energy harvesting based on a buckled beam. *Appl. Phys. Lett.* **2017**, *110*, 183903. [CrossRef]
153. Naseer, R.; Dai, H.L.; Abdelkefi, A.; Wang, L. Piezomagnetoelastic energy harvesting from vortex-induced vibrations using monostable characteristics. *Appl. Energy* **2017**, *203*, 142–153. [CrossRef]
154. Zhang, L.B.; Abdelkefi, A.; Dai, H.L.; Naseer, R.; Wang, L. Design and experimental analysis of broadband energy harvesting from vortex-induced vibrations. *J. Sound Vib.* **2017**, *408*, 210–219. [CrossRef]
155. Hou, C.; Shan, X.; Zhang, L.; Song, R.; Yang, Z. Design and Modeling of a Magnetic-Coupling Monostable Piezoelectric Energy Harvester Under Vortex-Induced Vibration. *IEEE Access* **2020**, *8*, 108913–108927. [CrossRef]
156. Wang, S.; Liao, W.; Zhang, Z.; Liao, Y.; Yan, M.; Kan, J. Development of a novel non-contact piezoelectric wind energy harvester excited by vortex-induced vibration. *Energy Convers. Manag.* **2021**, *235*, 113980. [CrossRef]
157. Hafizh, M.; Muthalif, A.G.A.; Renno, J.; Paurobally, M.R.; Mohamed Ali, M.S. A vortex-induced vibration-based self-tunable airfoil-shaped piezoelectric energy harvester for remote sensing applications in water. *Ocean Eng.* **2023**, *269*, 113467. [CrossRef]
158. Alimanesh, M.; Zamanian, M. Analysis of clamped-clamped piezoelectric energy harvester under vortex induced vibration considering the stretching effect. *J. Intell. Mater. Syst. Struct.* **2023**, *35*, 333–351. [CrossRef]
159. Li, Z.; Zhang, H.; Litak, G.; Zhou, S. Periodic solutions and frequency lock-in of vortex-induced vibration energy harvesters with nonlinear stiffness. *J. Sound Vib.* **2024**, *568*, 117952. [CrossRef]
160. Zhao, L.; Tang, L.; Yang, Y. Enhanced piezoelectric galloping energy harvesting using 2 degree-of-freedom cut-out cantilever with magnetic interaction. *Jpn. J. Appl. Phys.* **2014**, *53*, 060302. [CrossRef]
161. Bibo, A.; Alhadidi, A.H.; Daqaq, M.F. Exploiting a nonlinear restoring force to improve the performance of flow energy harvesters. *J. Appl. Phys.* **2015**, *117*, 045103. [CrossRef]
162. Zhou, Z.; Qin, W.; Zhu, P.; Shang, S. Scavenging wind energy by a Y-shaped bi-stable energy harvester with curved wings. *Energy* **2018**, *153*, 400–412. [CrossRef]
163. Tan, T.; Hu, X.; Yan, Z.; Zhang, W. Enhanced low-velocity wind energy harvesting from transverse galloping with super capacitor. *Energy* **2019**, *187*, 115915. [CrossRef]
164. Yang, K.; Wang, J.; Yurchenko, D. A double-beam piezo-magneto-elastic wind energy harvester for improving the galloping-based energy harvesting. *Appl. Phys. Lett.* **2019**, *115*, 193901. [CrossRef]
165. Wang, J.; Geng, L.; Zhou, S.; Zhang, Z.; Lai, Z.; Yurchenko, D. Design, modeling and experiments of broadband tristable galloping piezoelectric energy harvester. *Acta Mech. Sin. Xuebao* **2020**, *36*, 592–605. [CrossRef]
166. Sun, W.; Seok, J. Novel galloping-based piezoelectric energy harvester adaptable to external wind velocity. *Mech. Syst. Signal Process.* **2021**, *152*, 107477. [CrossRef]
167. Zhang, H.; Zhang, L.; Wang, Y.; Yang, X.; Song, R.; Sui, W. Modeling and experimental investigation of asymmetric distance with magnetic coupling based on galloping piezoelectric energy harvester. *Smart Mater. Struct.* **2022**, *31*, 065007. [CrossRef]
168. Ma, X.Q.; Zhang, H.; Margielewicz, J.; Gąska, D.; Wolszczak, P.; Litak, G.; Zhou, S.X. A dual-beam piezo-magneto-elastic wake-induced vibration energy harvesting system for high-performance wind energy harvesting. *Sci. China Technol. Sci.* **2023**, *67*, 221–239. [CrossRef]

169. Sousa, V.C.; De Melo Anicézio, M.; De Marqui Jr, C.; Erturk, A. Enhanced aeroelastic energy harvesting by exploiting combined nonlinearities: Theory and experiment. *Smart Mater. Struct.* **2011**, *20*, 94007. [CrossRef]
170. Bae, J.-S.; Inman, D.J. Aeroelastic characteristics of linear and nonlinear piezo-aeroelastic energy harvester. *J. Intell. Mater. Syst. Struct.* **2013**, *25*, 401–416. [CrossRef]
171. Wu, Y.; Li, D.; Xiang, J. Performance analysis and parametric design of an airfoil- based piezoaeroelastic energy harvester. In Proceedings of 56th AIAA/ASCE/AHS/ASC Structures, Structural Dynamics, and Materials Conference, Reston, VA, USA, 5–9 January 2015; pp. 1–13. [CrossRef]
172. Orrego, S.; Shoele, K.; Ruas, A.; Doran, K.; Caggiano, B.; Mittal, R.; Kang, S.H. Harvesting ambient wind energy with an inverted piezoelectric flag. *Appl. Energy* **2017**, *194*, 212–222. [CrossRef]
173. Wu, Y.; Li, D.; Xiang, J.; Da Ronch, A. Piezoaeroelastic energy harvesting based on an airfoil with double plunge degrees of freedom: Modeling and numerical analysis. *J. Fluids Struct.* **2017**, *74*, 111–129. [CrossRef]
174. Zhou, Z.; Qin, W.; Zhu, P.; Du, W.; Deng, W.; Pan, J. Scavenging wind energy by a dynamic-stable flutter energy harvester with rectangular wing. *Appl. Phys. Lett.* **2019**, *114*, 243902. [CrossRef]
175. Li, K.; Yang, Z.; Gu, Y.; He, S.; Zhou, S. Nonlinear magnetic-coupled flutter-based aeroelastic energy harvester: Modeling, simulation and experimental verification. *Smart Mater. Struct.* **2019**, *28*, 15020. [CrossRef]
176. Li, K.; Yang, Z.; Zhou, S. Performance enhancement for a magnetic-coupled bi-stable flutter-based energy harvester. *Smart Mater. Struct.* **2020**, *29*, 85045. [CrossRef]
177. Elahi, H.; Eugeni, M.; Lampani, L.; Gaudenzi, P. Modeling and Design of a Piezoelectric Nonlinear Aeroelastic Energy Harvester. *Integr. Ferroelectr.* **2020**, *211*, 132–151. [CrossRef]
178. Tian, H.; Shan, X.; Cao, H.; Song, R.; Xie, T. A method for investigating aerodynamic load models of piezoaeroelastic energy harvester. *J. Sound Vib.* **2021**, *502*, 116084. [CrossRef]
179. Tian, H.; Shan, X.; Cao, H.; Xie, T. Enhanced performance of airfoil-based piezoaeroelastic energy harvester: Numerical simulation and experimental verification. *Mech. Syst. Signal Process.* **2022**, *162*, 108065. [CrossRef]
180. Velusamy, V.R.; Foong, F.M.; Nik Mohd, N.A.R.; Thein, C.K. Bistable dual cantilever flutter for potential wind energy harvesting applications. *Sustain. Energy Technol. Assess.* **2024**, *63*, 103637. [CrossRef]
181. Li, Z.; Zhou, S.; Zhang, H.; Zhou, S. Periodic solutions and bifurcations of a tristable flutter-based energy harvester. *Aerosp. Sci. Technol.* **2024**, *144*, 108815. [CrossRef]
182. Fan, K.; Liu, S.; Liu, H.; Zhu, Y.; Wang, W.; Zhang, D. Scavenging energy from ultra-low frequency mechanical excitations through a bi-directional hybrid energy harvester. *Appl. Energy* **2018**, *216*, 8–20. [CrossRef]
183. Challa, V.R.; Prasad, M.G.; Fisher, F.T. A coupled piezoelectric-electromagnetic energy harvesting technique for achieving increased power output through damping matching. *Smart Mater. Struct.* **2009**, *18*, 095029. [CrossRef]
184. Zhao, J.; Zhang, H.; Su, F.; Yin, Z. A novel model of piezoelectric- electromagnetic hybrid energy harvester based on vortex-induced vibration. In Proceedings of the 2017 International Conference on Green Energy and Applications (ICGEA), Singapore, 25–27 March 2017; pp. 105–108. [CrossRef]
185. Rahman, M.T.; Salauddin, M.; Maharjan, P.; Rasel, M.S.; Cho, H.; Park, J.Y. Natural wind-driven ultra-compact and highly efficient hybridized nanogenerator for self-sustained wireless environmental monitoring system. *Nano Energy* **2019**, *57*, 256–268. [CrossRef]
186. Javed, U.; Abdelkefi, A. Characteristics and comparative analysis of piezoelectric-electromagnetic energy harvesters from vortex-induced oscillations. *Nonlinear Dyn.* **2019**, *95*, 3309–3333. [CrossRef]
187. Wang, Q.; Zou, H.-X.; Zhao, L.-C.; Li, M.; Wei, K.-X.; Huang, L.-P.; Zhang, W.-M. A synergetic hybrid mechanism of piezoelectric and triboelectric for galloping wind energy harvesting. *Appl. Phys. Lett.* **2020**, *117*, 43902. [CrossRef]
188. Li, Z.; Li, X.; Liu, B.; Wang, J. Influence of vehicle body vibration induced by road excitation on the performance of a vehicle-mounted piezoelectric-electromagnetic hybrid energy harvester. *Smart Mater. Struct.* **2021**, *30*, 55019. [CrossRef]
189. Al-Riyami, M.; Bahadur, I.; Ouakad, H. There Is Plenty of Room inside a Bluff Body: A Hybrid Piezoelectric and Electromagnetic Wind Energy Harvester. *Energies* **2022**, *15*, 6097. [CrossRef]
190. Li, Z.; Zhou, S.; Li, X. A piezoelectric–electromagnetic hybrid flutter-based wind energy harvester: Modeling and nonlinear analysis. *Int. J. Non. Linear. Mech.* **2022**, *144*, 104051. [CrossRef]
191. Li, X.; Ma, T.; Liu, B.; Wang, C.; Su, Y. Experimental Study on Magnetic Coupling Piezoelectric–Electromagnetic Composite Galloping Energy Harvester. *Sensors* **2022**, *22*, 8241. [CrossRef]
192. Mannini, C.; Marra, A.M.; Massai, T.; Bartoli, G. Interference of vortex-induced vibration and transverse galloping for a rectangular cylinder. *J. Fluids Struct.* **2016**, *66*, 403–423. [CrossRef]
193. Hu, G.; Tse, K.T.; Wei, M.; Naseer, R.; Abdelkefi, A.; Kwok, K.C.S. Experimental investigation on the efficiency of circular cylinder-based wind energy harvester with different rod-shaped attachments. *Appl. Energy* **2018**, *226*, 682–689. [CrossRef]
194. He, X.; Yang, X.; Jiang, S. Enhancement of wind energy harvesting by interaction between vortex-induced vibration and galloping. *Appl. Phys. Lett.* **2018**, *112*, 033901. [CrossRef]
195. Petrini, F.; Gkoumas, K. Piezoelectric energy harvesting from vortex shedding and galloping induced vibrations inside HVAC ducts. *Energy Build.* **2018**, *158*, 371–383. [CrossRef]
196. Qin, W.; Deng, W.; Pan, J.; Zhou, Z.; Du, W.; Zhu, P. Harvesting wind energy with bi-stable snap-through excited by vortex-induced vibration and galloping. *Energy* **2019**, *189*, 116237. [CrossRef]

197. Wang, J.; Gu, S.; Zhang, C.; Hu, G.; Chen, G.; Yang, K.; Li, H.; Lai, Y.; Litak, G.; Yurchenko, D. Hybrid wind energy scavenging by coupling vortex-induced vibrations and galloping. *Energy Convers. Manag.* **2020**, *213*, 112835. [CrossRef]
198. Tian, H.; Yurchenko, D.; Li, Z.; Guo, J.; Kang, X.; Wang, J. Dumbbell-shaped piezoelectric energy harvesting from coupled vibrations. *Int. J. Mech. Sci.* **2024**, *281*, 109681. [CrossRef]
199. Ding, L.; Mao, X.; Yang, L.; Yan, B.; Wang, J.; Zhang, L. Effects of installation position of fin-shaped rods on wind-induced vibration and energy harvesting of aeroelastic energy converter. *Smart Mater. Struct.* **2021**, *30*, 025026. [CrossRef]
200. Xing, J.; Rezaei, M.; Dai, H.; Liao, W.-H. Investigating the coupled effect of different aspect ratios and leeward protrusion lengths on vortex-induced vibration (VIV)-galloping energy harvesting: Modelling and experimental validation. *J. Sound Vib.* **2024**, *568*, 118054. [CrossRef]
201. Chen, S.; Wang, C.H.; Zhao, L. A two-degree-of-freedom aeroelastic energy harvesting system with coupled vortex-induced-vibration and wake galloping mechanisms. *Appl. Phys. Lett.* **2023**, *122*, 63901. [CrossRef]
202. Shan, X.; Tian, H.; Cao, H.; Xie, T. Enhancing Performance of a Piezoelectric Energy Harvester System for Concurrent Flutter and Vortex-Induced Vibration. *Energies* **2020**, *13*, 3101. [CrossRef]
203. Li, X.; Wang, X.; Tian, H.; Wang, C.; Liu, B. Experimental Research of Symmetrical Airfoil Piezoelectric Energy Harvester Excited by Vortex-Induced Flutter Coupling. *Appl. Sci.* **2022**, *12*, 12514. [CrossRef]
204. Wan, C.; Tian, H.; Shan, X.; Xie, T. Enhanced performance of airfoil-based piezoelectric energy harvester under coupled flutter and vortex-induced vibration. *Int. J. Mech. Sci.* **2023**, *241*, 107979. [CrossRef]
205. Fu, H.; Mei, X.; Yurchenko, D.; Zhou, S.; Theodossiades, S.; Nakano, K.; Yeatman, E.M. Rotational energy harvesting for self-powered sensing. *Joule* **2021**, *5*, 1074–1118. [CrossRef]
206. Zhang, J.; Fang, Z.; Shu, C.; Zhang, J.; Zhang, Q.; Li, C. A rotational piezoelectric energy harvester for efficient wind energy harvesting. *Sens. Actuators A Phys.* **2017**, *262*, 123–129. [CrossRef]
207. Fan, X.; He, J.; Mu, J.; Qian, J.; Zhang, N.; Yang, C.; Hou, X.; Geng, W.; Wang, X.; Chou, X. Triboelectric-electromagnetic hybrid nanogenerator driven by wind for self-powered wireless transmission in Internet of Things and self-powered wind speed sensor. *Nano Energy* **2020**, *68*, 104319. [CrossRef]
208. Li, B.; Qiu, Y.; Huang, P.; Tang, W.; Zhang, X. Self-powered forest ambient monitoring microsystem based on wind energy hybrid nanogenerators. *Sci. China Technol. Sci.* **2022**, *65*, 2348–2360. [CrossRef]
209. Egbe, K.-J.I.; Matin Nazar, A.; Jiao, P. Piezoelectric-triboelectric-electromagnetic Hybrid Rotational Energy Harvesters (H-REH). *Int. J. Mech. Sci.* **2022**, *235*, 107722. [CrossRef]
210. Narolia, T.; Mandaloi, G.; Gupta, V.K. Design and experimental analysis of low wind speed rotary piezoelectric energy harvester. *Int. J. Mech. Mater. Des.* **2023**, *19*, 793–804. [CrossRef]
211. Cao, X.; Zhou, H.; Zhou, Y.; Hu, Y.; Wang, Y.; Wang, Z.L.; Sun, Q. High Performance Rotary-Structured Triboelectric-Electromagnetic Hybrid Nanogenerator for Ocean Wind Energy Harvesting. *Adv. Mater. Technol.* **2023**, *8*, 2300327. [CrossRef]
212. Li, J.; Wang, G.; Yang, P.; Wen, Y.; Zhang, L.; Song, R.; Hou, C. An orientation-adaptive electromagnetic energy harvester scavenging for wind-induced vibration. *Energy* **2024**, *286*, 129578. [CrossRef]
213. Li, Y.; Deng, H.; Wu, H.; Luo, Y.; Deng, Y.; Yuan, H.; Cui, Z.; Tang, J.; Xiong, J.; Zhang, X.; et al. Rotary Wind-driven Triboelectric Nanogenerator for Self-Powered Airflow Temperature Monitoring of Industrial Equipment. *Adv. Sci.* **2024**, *11*, 2307382. [CrossRef]